# Generation of Mesenchymal Stem Cells Expressing Islet Neogenesis-Associated Protein (INGAP)

By

Shaun D. Violette-Deslauriers

Department of Surgery, Division of Surgical Research
McGill University
Montreal

July 2017

A thesis submitted to McGill University in partial fulfillment of the requirements of the degree of Master of Science

© Shaun David Violette-Deslauriers 2017

## ABSTRACT

Beta cell death is responsible for the pathogenesis of both Type-1 and Type-2 diabetes patients. Pancreatic beta cell regeneration, either through the induction of beta cell proliferation, or through beta cell neogenesis resulting from the differentiation of other cell types, is becoming an attractive prospect for achieving a true curative therapy. Islet Neogenesis-Associated Protein (INGAP), previously identified by Dr. Lawrence Rosenberg, has been documented to promote beta cell regeneration and improved glucose tolerance in animal models. A peptide derivative of INGAP has shown similar effects and is currently undergoing phase II clinical trials. We hypothesize that the effects of INGAP can be improved by continuous *in vivo* release, which can be achieved through secretion of INGAP by an implanted cell population. Mesenchymal stem cells (MSCs) represent a promising choice for INGAP delivery, owing to their advantageous "homing", regenerative and immunomodulatory properties, as well as the many benefits they have exhibited when injected into both diabetic animals and human patients. In this study, to prove that MSCs can express and secrete INGAP, C57BL/6 mouse bone marrow-derived mesenchymal stem cells were transfected with a plasmid encoding INGAP cDNA. The expression and secretion of INGAP in these cells was then confirmed both by Western Blot of conditioned media, and by fluorescence microscopy. To further optimize the detectability of secreted INGAP for use in animal studies, a new DDK (FLAG) tagged INGAP cDNA construct was designed, using a sub-cloning approach. In addition, INGAP-DDK cDNA was incorporated into a retroviral plasmid for the generation of retroviral particles for transduction applications. These experimental results demonstrate that the cellular machinery of MSCs is capable of secreting full length INGAP, and lay the foundation for producing reliable INGAP-expressing MSCs through viral transduction, for use in future *in vitro* and *in vivo* experimentation.

## RÉSUMÉ

La mort des cellules bêta est à l'origine de la pathogénèse du diabète de Type 1 et de Type 2. La regénération de ces cellules, soit par la prolifération de cellules bêta existantes, ou par la neogénèse résultant de la différenciation de cellules provenant d'autres lignées, devient une proposition intéressante pour obtenir une véritable thérapie curative. L'injection de l' "Islet Neogenesis-Associated Protein" (INGAP), identifiée par le Dr. Lawrence Rosenberg, a réussi à promouvoir la regénération de cellules bêta, et à améliorer la tolérence au glucose, chez des animaux. Un peptide, dérivé de INGAP, a produit des effets comparables, et est couramment sous investigation dans le contexte d'études cliniques de phase II. On soumet l'hypothèse que les effets d'INGAP peuvent êtres accrus par une relache continue *in vivo*, ce qui peut etre accompli par la sécretion d'INGAP au moyen de cellules implantées. Les cellules souches mésenchymateuses (MSCs), derivées de la moelle osseuse, constituent un excellent choix pour la livraison d'INGAP, à cause de leurs propriétés regénératrices, immunomodulatrices, et migratrices, ainsi que les bénéfices préalables qu'elles ont apporté au cours d'études où elles ont été injectées chez des animaux et des patients humains. Au cours d'étude présenté ici, pour établir que les MSCs peuvent exprimer et sécéter INGAP, des MSCs de souris C57Bl/6 ont été transfectées en utilisant un plasmide contenant l'ADNc de INGAP. L'expression et la sécretion d'INGAP dans ces cellules ont ensuite été confirmé par Western Blot et par immunofluoréscence. Pour optimizer la détection d'INGAP, en vue d'études futures sur des animaux, un nouveau plasmide contenant un marqueur DDK (FLAG) a été construit, utilisant une approche de sous-clonage. De plus, la portion INGAP-DDK a été introduit dans un plasmide rétroviral, pour servir à des applications futures de transduction rétrovirale. Ces résultats expérimentaux démontrent que la machinerie céllulaire des MSCs est capable de sécréter une

protéine INGAP de pleine longueur, et établissent la base d'une méthode fiable pour la génération de MSCs exprimant INGAP, qui pourront servir au cours d'études subséquentes *in vitro* et *in vivo*.

## ACKNOWLEDGEMENTS

I would first like to thank **Dr. Lawrence Rosenberg** and **Dr. Nicoletta Eliopoulos** for welcoming me into their research teams and entrusting me with this project. They provided a friendly work environment, as well as the guidance with which to overcome the hurdles inherent to scientific pursuits.

Thank you to the members of my supervisory committee: **Dr. Fackson Mwale, Dr. Jun-Li Liu,** and **Dr. Arezu Jahani** for their feedback and suggestions which have helped guide the writing of this thesis.

Special thanks go out to my colleagues, both in the Rosenberg and Eliopoulos labs: to **Dr. Maria Petropavlovskaia**, whose knowledge and expertise have proved indispensable to this excellent learning experience; to **Dr.Beatrice Assouline**, for teaching me many of the laboratory techniques I still use every day; and to **Jing Zhao**, and **Jessica Cuerquis** for their continued mentorship and helpful troubleshooting advice.

I would also like to thank others who have contributed to my time here at the LDI and as a student of experimental surgery: to **Barbara Reney** and **Sharon Turner**, who have always set time aside to help me with supporting documentation, and to **Christian Young**, for teaching me to use the automated cell counter. Thank you to **Eni Nano**, **Malak Ismail** and **Steve Leghost** for their support and entertaining lunchtime banter.

Most importantly, thank you to my parents, Michele and Ben, whose encouragement has allowed me to become who I am today.

## LIST OF TABLES

## LIST OF FIGURES

# LIST OF ABBREVIATIONS

| | |
|---|---|
| **ATP** | adenosine triphosphate |
| **BSA** | bovine serum albumin |
| **cDNA** | complementary deoxyribonucleic acid |
| **CMV** | cytomegalovirus |
| **CY3** | cyanine 3 |
| **CHO** | Chinese hamster ovary |
| **Cos-1** | African Green Monkey kidney |
| **DEPC** | diethyl pyrocarbonate |
| **EDTA** | ethylenediaminetetraacetic acid |
| **EGF** | epidermal growth factor |
| **EGFR** | epidermal growth factor receptor |
| **ELISA** | enzyme-linked immunosorbent assay |
| **EPO** | erythropoietin |
| **ESC** | embryonic stem cell |
| **GAD65** | glutamic acid decarboxylase 65 |
| **GFP** | green fluorescent protein |
| **GLP-1** | glucagon-like peptide-1 |
| **GLUT 2** | glucose transporter 2 |
| **GPCR** | G-protein coupled receptor |
| **HLA** | heuman leukocyte antigen |
| **HPDE** | human pancreatic ductal epithelial |
| **HRP** | horseradish peroxidase |
| **IA2** | islet antigen 2 |
| **INGAP** | islet neogenesis-associated protein |
| **INGAP-P** | INGAP-peptide |
| **IRES** | internal ribosomal entry site |
| **iPSC** | induced pluripotent stem cell |
| **LB** | lysogeny broth |
| **MAPK** | mitogen-activated protein kinase |
| **mRNA** | messenger ribonucleic acid |
| **MSC** | mesenchymal stem cells |
| **NOD** | non-obese diabetic |
| **PBS** | phosphate-buffered saline |
| **PCR** | polymerase chain reaction |
| **PPP** | pancreatic polypeptide |
| **qPCR** | quantitative polymerase chain reaction |
| **REG** | regulatory Protein |
| **RIN** | rat insulinoma |
| **SDS-PAGE** | sodium dodecyl sulfate polyacrylamide gel electrophoresis |
| **STZ** | streptozotocin |
| **TBST** | tris-buffered saline + tween20 |
| **T1DM** | type-1 diabetes mellitus |
| **T2DM** | type-2 diabetes mellitus |

## TABLE OF CONTENTS

## CHAPTER 2 : METHODS



## CHAPTER 3 : RESULTS

## CHAPTER 4 : DISCUSSION

# CHAPTER 1: INTRODUCTION

## 1.1 THE PANCREAS

The pancreas, a mammalian abdominal organ adjacent to the duodenum and spleen, is responsible for essential endocrine and exocrine functions: from aiding digestion to regulating glucose metabolism [1, 2]. It is supplied by the celiac and superior mesenteric arteries, and drained by the splenic and superior mesenteric veins which lead into the portal vein [3-5]. Innervation is supplied sympathetically: to the hepatic and celiac plexuses, and parasympathetically: through the vagus nerve to the inter-pancreatic ganglia [6, 7]. The majority of the pancreas's volume is dedicated to the production and delivery of exocrine products, and is populated by enzyme-producing acinar cells, paired with small ductules [8]. Digestive enzymes and bicarbonate, produced by the acinar cells, travel through the ductules to the main pancreatic duct [9]. Union of the pancreatic duct to the common bile duct then allows for the release of these exocrine products into the duodenum via the duodenal papilla [10, 11]. The pancreatic enzymes are stored within zymogen granules while in the acinar cells, and remain inactive until they encounter activating factors (mainly enterokinase) in the intestinal brush border of the duodenal lumen, to avoid auto-digestion [9]. Quantity and frequency of enzymatic production are indirectly regulated in response to dietary intake and bolus composition [12]. Small endocrine masses known as the Islets of Langerhans, making up less than 20% of pancreatic tissue, serve the organ's critical endocrine functions [8, 13, 14].

## 1.2 THE ISLETS OF LANGERHANS

Pancreatic islets are distributed throughout the organ, and consist of highly vascularized endocrine cell clusters [13, 15]. Five major cell types contribute, with varying degrees, to islet composition: Alpha cells produce the glucagon hormone; Beta cells produce the insulin hormone, an antagonist to glucagon; Delta cells produce somatostatin; Gamma cells produce pancreatic polypeptide; and Epsilon cells produce ghrelin [16]. Both insulin and glucagon are critical to glucose homeostasis and metabolism, while somatostatin constitutes a trophic hormone, indirectly regulating the release of neurotransmitters and other hormones. Pancreatic polypeptide regulates both endocrine and exocrine pancreatic functions through feedback inhibition, and ghrelin plays a role, both in growth hormone release, and in increasing appetite in response to gastric emptying [16]. Islet organization and sub-structure can vary significantly between species. In humans, both alpha and beta cells are observed throughout the islet area, while in mice, beta cells tend to present themselves as a more central mass surrounded by peripheral alpha cells [17]. Human islet physiology favors alpha-alpha and alpha-beta cell contact while maintaining proximity of endocrine cells to blood vessels [18]. The size of individual islets is conserved between species, although islet mass, and therefore total islet number increases proportionally to body weight to meet the increased insulin demands in larger animals [17].

## 1.3 BLOOD GLUCOSE HOMEOSTASIS & METABOLISM

Dietary carbohydrates are consumed primarily in the form of polysaccharides such as starch (amylose and amylopectin) and dextrins, and a variety of monosaccharides (glucose,

fructose, and galactose) and disaccharides (sucrose, lactose, and maltose) [19, 20]. Polysaccharides are rapidly digested by salivary amylase and pancreatic α-amylase into maltose, maltotriose, isomaltose, lactose and α-limit dextrins as they descend from the mouth to the small intestine [19, 20]. These, along with other dietary oligosaccharides, undergo further digestion in the glycocalyx layer of the intestinal brush border to produce glucose and fructose, which can then be absorbed through the intestinal epithelium, and into the bloodstream, along with any glucose, fructose or galactose already present in the diet [19, 20]. These monosaccharides travel to the liver via the hepatic portal vein, where a significant portion of the fructose and galactose is converted into glucose: the major end product of carbohydrate digestion [19, 20]. It is at this point that two antagonist pancreatic endocrine hormones: Insulin and Glucagon, act to regulate the levels of glucose present in the bloodstream [16].

Bodily tissues are in constant demand for energy, and therefore for glucose [19, 20]. Some tissues, such as the brain and liver, can import glucose from the bloodstream without the action of insulin, as they require large amounts of glucose even in the fasted state [21, 22]. However, the majority of tissues, such as muscle and adipose, primarily utilize an insulin-dependent glucose uptake mechanism, as they convert excess glucose into glycogen, a polysaccharide unique to animal metabolism which acts as a form of glucose storage during the fed state [21, 23]. In the event of an elevated blood glucose level, such as following a meal, where the amount of glucose introduced into circulation exceeds immediate physiological demands, insulin will act to favor its uptake by adipose, muscle, and liver cells, followed by subsequent conversion into glycogen: [16, 20, 24]. However, between meals, as the blood glucose levels drop, glucagon will induce glycogenolysis, the breakdown of glycogen into

glucose, and the release of glucose back into the bloodstream, so that it is available to meet physiological energy needs [16, 20, 24].

### 1.3.1 BLOOD GLUCOSE SENSING MECHANISMS

Insulin hormone is secreted by beta cells in direct response to elevated blood glucose levels. High expression of Glut 2 glucose transporters allows rapid entry of glucose into these cells, where it undergoes phosphorylation to glucose-6-phosphate, mediated by GK hexokinase IV, in the first step of glycolysis [21, 25]. The rate at which this phosphorylation step occurs is hypothesized to function as a glucose sensing mechanism, regulating insulin release [26]. Pyruvate, the end product of glycolysis, is thought to also provide a degree of feedback, further governing insulin release [26]. In addition to metabolic glucose detection mechanisms, the depolarization of beta cell membranes resulting from elevated intracellular glucose is capable of triggering action potentials, which in turn cause influx of calcium ions [27, 28]. Elevated cellular calcium levels trigger vesicle exocytosis, and therefore promotes the release of insulin granules, although a variety of other signals are necessary to insure the adequate production and mobilization of insulin granules, so that they may be ready for release [26-28]. Control of insulin release, and of its antagonist, glucagon, cannot be attributed to a single mechanism, but results from interactions between direct glucose sensing mechanisms, hormonal signaling and neural stimulus [25].

## 1.4 DIABETES MELLITUS

### 1.4.1 PATHOPHYSIOLOGY OF TYPE 1 DIABETES

Diabetes Mellitus was initially characterized by a dramatic increase in urination frequency (polyuria) and thirst (polydipsia), followed by a rapid decline in body weight and muscle mass, eventually leading to coma and death [29]. These symptoms were compounded upon the consumption of starchy food, or any food high in glucose or glucose precursors [29]. The etiology of this disease, now defined as Type 1 diabetes mellitus (T1DM), is the rapid decline of insulin-producing beta cell mass in response to autoimmune-mediated destruction [30]. As in other autoimmune diseases, a single root cause is difficult to identify. An array of genetic and epigenetic traits compound to cause failures in the body's tolerance mechanisms, which act to eliminate immune cells recognizing autoantigens under normal healthy circumstances [31]. Tolerance is divided into two principle categories: central tolerance, which prevents autoreactive immune cell precursors from maturing; and a failsafe mechanism known as peripheral tolerance, which acts to quickly neutralize circulating autoreactive cells which bypassed the central tolerance process [31, 32]. In individuals with T1DM, CD4+ and CD8+ T-cells reactive to islet antigens bypass both tolerance mechanisms, and therefore recognize the pancreatic beta cell as foreign, acting directly and recruiting macrophages to destroy them [33-35]. Many of these beta cell antigens have been identified. The most common include: GAD65, IA2, and insulin itself [36]. Once the autoimmune process begins, symptoms appear very rapidly, and the majority of pancreatic beta cells are destroyed within a few weeks [29, 30].

## 1.4.2 PATHOPHYSIOLOGY OF TYPE 2 DIABETES

Within the past century, the incidence of Type 1 Diabetes has been rapidly superseded by a second form of the disease, Type 2 diabetes (T2DM) [37]. In contrast to T1DM, the type 2 variant ensues, not from initial islet destruction, but from peripheral cellular resistance to the actions of insulin [38]. This peripheral resistance is often due to an accumulation of cellular lipid droplets as a result of obesity, or inflammation [38, 39]. In effect, the dramatic increase in T2DM incidence has been directly linked to the widespread, and ever increasing, prevalence of obesity [38]. As insulin becomes incapable of stimulating cellular glucose uptake, blood glucose rises, stimulating a feedback loop which increases demand for insulin [40]. If this state is maintained, the excessive strain placed upon the beta cell population leads to hypertrophy [40, 41]. In adults over the age of 30, beta cell proliferation rates are exceptionally low, further impeding potential recovery or compensation [42]. Both forms of the disease, T1DM and T2DM, therefore lead to the eventual depletion or insufficiency of beta cell mass, although this occurs much more rapidly in Type-1, and can be delayed in Type-2 by strict management of diet and exercise, and through adherence to prescribed treatments [30, 38, 43, 44].

## 1.4.3 DIABETIC COMPLICATIONS

Few diabetic complications present immediately, although these can rapidly become fatal if left untreated [45]. Ketoacidosis results from a lack of circulating insulin, which inhibits cellular glucose intake, shifting metabolism away from glycolysis towards fatty acid breakdown, and causing an extreme hyperglycemia [46]. A byproduct of this reaction is the formation of ketone bodies which can rapidly and dangerously acidify blood when present in excess [46]. In

the reverse state, extreme hypoglycemia, brain tissue glucose demands go unmet, leading to cell death, and very rapidly plunges the affected individual into a coma, leading to death [47]. However, the majority, and most debilitating, of diabetic complications stem from body-wide damage to the micro and macrovasculature from prolonged exposure to elevated blood glucose levels, and can take many years to develop [45]. Potential microvascular complications consist of: retinopathy, nephropathy, and neuropathy, which can respectively result in: blindness, kidney failure, and loss of peripheral nerve sensitivity [45, 48]. Potential macrovascular complications consist of accelerated arterial atherosclerosis, which results in strokes or myocardial infarcts [45, 48]. Additionally, the combination of diabetic neuropathy and microvascular damage can cause necrosis of the extremities, potentially necessitating limb amputation [45, 49]. Although good disease management and treatment adherence help prevent the onset of these complications, many recent findings point out that even ideal blood glucose management does not rule out their advent [50]. Studies suggest that exogenous insulin injections, while restoring a semblance of normoglycemia, do not provide circulating C-peptide, the byproduct of natural insulin production [50, 51]. C-peptide has been shown to play an important role in the prevention of atherosclerosis [50-52].

## 1.5 SOCIOECONOMIC IMPACT OF DIABETES

Diabetes Mellitus is one of the top five most prevalent non-communicable diseases. It affects 7.8% of Canadians and contributes to 3.8% of all deaths [53]. For the year 2015, Seurig et al. established the annual per-capita cost of diabetes in Canada to be between 2000 and 3000$ [54]. In the USA, this cost per capita exceeds 6000$ per year [54]. A worldwide study of the

economic impact of diabetes completed in 2016 has established that total diagnosed cases of diabetes in adults currently exceed 420 million. This represents a global annual treatment cost of 825 billion international dollar equivalent, and a 400% increase since 1980 [55]. Predictive models from this same study estimate that over 700 million adults could be affected by the year 2025 [55]. However, this does not yet take into account the significant proportion of individuals who may have undiagnosed Type 2 Diabetes, especially in low income countries where access to healthcare is limited.

## 1.6 CURRENT THERAPIES FOR DIABETES

### 1.6.1 INSULIN-BASED THERAPIES

The lack of circulating blood insulin levels as seen in Type 1 diabetes and severe late stage Type 2 diabetes has been addressed almost exclusively with exogenous insulin injections since its discovery in 1922 [56-58] . While the fundamental approach has remained the same, numerous advancements have been made in both the composition and dosage of injectable insulin to achieve blood glucose regulation that more closely mimics normal physiological release patterns [57]. First attempts consisted of canine pancreatic extracts, which quickly gave way to other more readily available animal sources, primarily of the porcine variety [56, 59]. The potency of these insulin extracts was soon increased using an isoelectric purification method, while the duration of effects was found to be increased by the addition of protamine and zinc [56, 58, 60, 61]. Insulin became the first commercially synthetized human protein through recombinant production by bacterial strains (E-coli) in the early 1980s [62, 63]. This new, less immunoreactive form of insulin was christened and marketed as “humulin” [59]. Most recent

efforts focus on alternative routes of insulin delivery to improve release profiles and practicality [57]. Rapid technological developments allowed for miniaturization of automated insulin pumps throughout the last decade, with experimental applications using subdermal implants [64, 65]. Transdermal insulin delivery through a cutaneous patch, inhalable insulin atomizers, and various alternatives for oral delivery are also undergoing development [66-69].

### 1.6.2 PHARMACOLOGICAL THERAPIES

Patients affected by T2DM retain a larger beta cell mass than those affected by T1DM [38, 40]. Treatment plans for the Type-2 variant therefore begin, aside from diet and exercise regimens, with oral pharmaceuticals, and traditionally only move towards insulin therapy if these patients are unresponsive to previous efforts [70]. Current pharmaceutical therapies can be divided into three principal categories: Sensitizers, which include Biguanides and Thiazolidinediones; Secretagogues, which include Sulfonylureas and Meglitinides; and Alpha-Glucosidase inhibitors [71]. Biguanides, such as Metformin, present a variety of physiological effects such as: decreased intestinal glucose absorption and hepatic gluconeogenesis, decreased fatty acid oxidation, and increased peripheral insulin sensitivity [71, 72]. Thiazolidinediones reduce circulating free fatty acid levels by activating peroxisome proliferator-activated nuclear receptors which act as transcription modifiers, resulting in a shift from fatty acid metabolism towards carbohydrate/glucose metabolism [71, 73]. Sulfonylureas stimulate the release of insulin granules by increasing membrane depolarization in remaining beta cells through the inhibition of ATP-dependant K+ channels, and decrease clearance of insulin from the bloodstream by the liver [74, 75]. Meglitinides, which include benzoic acid derivatives and D-

phenylalanine derivatives, serve the same basic function as Sulfonylureas, but act more rapidly and bind an alternate receptor acting upon ATP-dependant K+ channels [71, 76]. Finally, Alpha-Glucosidase inhibitors (acarbose, miglitol & voglibose), as the name suggests, inhibit α-glucosidase in the intestinal brush border, thereby preventing the conversion of partially digested disaccharides into absorbable monosaccharides [77].

Incretin Mimetics constitute a recent addition to available diabetic pharmacological therapies, although they are administered as injectables, not through oral delivery [78]. These peptides function by imitating and binding to receptors normally reserved for incretins, such as GLP-1: a class of hormones responsible for enhancing the strength of insulin release in response to increased glucose levels [78, 79]. Overall, Incretin mimetics result in increased insulin production and release, and decreased glucagon release and gastric emptying [79].

### 1.6.3 TRANSPLANTATION BASED THERAPIES

The discovery of injectable insulin allowed patients with T1DM to survive in the face of an otherwise lethal disease, but required a strict control of injection times and doses, and in some patients caused susceptibility to extreme hypoglycemias [56, 80]. The first successful whole pancreas transplantation occurred in 1966, with the goal of treating patients less responsive to insulin therapy [81]. While efficient at reversing the pathological condition, as demonstrated by increased glucose tolerance and circulating insulin and C-peptide concentrations, this procedure comes at the expense of potent immunosuppressive therapy, due to the allogeneic nature of the graft, and the difficulty of obtaining HLA matched donor tissue [82, 83]. Despite numerous advancements in exogenous insulin therapy, whole pancreas transplantation is still utilized to this day, in the most severe cases of diabetes, but principally in patients who are already subject to

immunosuppression therapy for the maintenance of other grafts, such as transplanted kidneys [81, 84]. It has been reported that pancreatic graft survival is significantly higher when transplanted simultaneously with a kidney from the same donor: 87.3% after one year, in comparison to 82.5% for pancreas-only transplants [84, 85].

The first successful human islet transplantations, as opposed to whole pancreas transplantation, to result in long-term diabetes reversal were conducted in 1999, following the advent of an effective pancreatic islet isolation method known as the Edmonton protocol [86]. A principal advantage of this technique is reduced volume of foreign tissue introduced, thereby reducing invasiveness, replacing only the damaged islets while allowing the patient to maintain their native pancreatic exocrine functions [87]. As in the case of whole pancreas transplantation, this therapy is most often best suited to patients with Type 1 diabetes who respond poorly to conventional insulin therapy, but also requires potent immunosuppressant therapy [87]. Even in the absence of graft rejection, only approximately 60% of recipients achieve insulin independence outright [88, 89]. In addition, 56% of these islet recipients do not maintain insulin independence within the first five years following the procedure, but do retain some benefits with regards to glucose tolerance and a reduction in hypoglycemia frequency following insulin injection [88, 89].

## 1.7 PANCREATIC REGENERATION

### 1.7.1. POTENTIAL SOURCES FOR NEW BETA CELLS

Breakthroughs in the field of developmental biology have paved the way towards a better understanding of beta cell origin and differentiation. Consequently, regenerative therapies are

increasingly under investigation as a means of replenishing beta cell mass, as they benefit from approaches that more closely approximate normal development. Adult beta cells had long been considered incapable of replication following initial embryonic development [90]. However, ever increasing evidence points to the plasticity of pancreatic islet number, composition and morphology, especially in response to physiological stressors such as diabetes, obesity or pregnancy, which primarily affect beta cell mass [91]. Beta cells are now known to have a slow mitotic rate in healthy adults, which translates to a mitotic index of approximately 2.5% in rodents, and only 0.2% in humans, although proliferation may be increased in response to the aforementioned physiological stressors [42].

Many studies have also examined the potential for other cells to transdifferentiate into fully functioning beta cells [92]. The first likely candidates are other islet cells, which develop from the same lineage as the beta cell during fetal growth [93, 94]. Approximately 1-3% of endogenous alpha cells were found to secrete both insulin and glucagon within one day after the onset of near-total beta cell destruction, triggered by the administration of diphtheria toxin in transgenic mice encoding the diphtheria toxin receptor sequence bound to an insulin promoter [95]. Lineage tracing of alpha cells using the Cre-*lox*P system further identified a high rate of alpha-beta transdifferentiation, where 65% of new beta cells present one month after near-total ablation were found to originate from alpha cells [95]. A study later performed by Chera et al. found that new beta cells can also arise from the transdifferentiation of delta cells in prepubertal mice [96].

Transdifferentiation of acinar cells represents another possible source of beta cells. Spherical clusters of rat acinar cells, cultured for one week in suspension, were observed to acquire ductal cell-like morphology, while cells at the cluster's periphery began to secrete insulin

[97]. *In vitro* culture of acinar cells from Streptozotocin treated mice, in the presence of epidermal growth factor and nicotinamide, has also been shown to induce the expression of pancreatic endocrine products: Insulin, Glucagon, Somatostatin and Pancreatic Polypeptide (PPP) [98]. Further studies using this protocol have achieved an approximate 5% acinar to beta-like cell conversion rate, also confirming the exocrine origin of the observed cells using Cre/loxP lineage tracing [99].

Finally, pancreatic islets develop from the ductal epithelium during embryogenesis and are therefore close relatives to ductal epithelial cells, leading many studies to examine the potential for ductal to islet cell transdifferentiation [100]. *In vitro* monolayer culture of human ductal epithelial cells overlayed with matrigel yielded the formation of islet-like clusters which tested insulin-positive after 3-4 weeks [101]. In spite of these promising results, natural recovery processes are observably too slow to counter severe pathologies such as diabetes in humans. The exogenous stimulation of neogenic processes therefore represents a promising therapeutic approach.

## 1.7.2 REGENERATIVE AGENTS

Various compounds have been proposed to stimulate beta cell regeneration. These can generally be divided into two categories: those stimulating the proliferation of existing beta cells, and those promoting the reprogramming of other cells towards the beta cell fate [102]. WS6 is a promising proliferative agent which can induce the expansion of both beta and alpha cells in *in vitro* human islet cultures without negatively impacting overall islet viability [103, 104]. Similarly, 5-iodotubercidin constitutes a second example of mitogens which can induce human

beta cell proliferation, this time both in culture and *in vivo*, through inhibition of adenosine kinase receptors [102, 105].

Other molecules can guide cell reprogramming towards the beta cell fate. Indolactam V stimulates the differentiation of cultured induced pluripotent stem cells (iPSCs) and embryonic stem cells (ESCs) towards beta cell-like lineages [106, 107]. Co-administration of epidermal growth factor (EGF) and Gastrin can produce up to a 3-fold beta cell mass increase in diabetic mice, both through beta cell proliferation and neogenesis, as demonstrated by lineage tracing [108]. Proliferation of beta cells has been found to be partially dependant on the presence of epidermal growth factor receptor 1 (EGFR) [109]. Other epidermal growth factor receptors (ErbB-1 and ErbB-4) can be activated by Betacellulin, a member of the EGF family which also exerts both proliferative and neogenic effects upon the beta cell population [110]. Administration of Gastrin alone has previously yielded a two-fold increase in beta cell mass in rats rendered diabetic by partial duct ligation, where a high amount of acinar-to-beta cell transdifferentiation was known to occur [111]. Some incretin mimetics, such as Glucagon-Like Peptide-1 (GLP-1), which are frequently administered as oral pharmaceutical therapy in type-2 diabetics, are thought to promote alpha-to-beta trans-differentiation in addition to proliferative effects upon beta cells [112-114].

### 1.7.3 ISLET NEOGENESIS-ASSOCIATED PROTEIN (INGAP)

The obstruction of hamster pancreatic ducts using cellophane wrapping was previously found to produce an increase in beta cell mass, with many new islets arising as duct-associated structures, indicating that neogenic processes were also being stimulated [115, 116]. Following

this observation, protein extracts (named ilotropin) from obstructed pancreata were found to greatly reduce diabetic symptoms in chemically-induced (streptozotocin treated) diabetic hamsters [117]. A 16.8kD protein, was isolated through differential display of mRNA from obstructed and non-obstructed pancreas samples, by Rafaeloff et al., and subseqently named "Islet Neogenesis-Associated Protein" or "INGAP" [117].

The effects of INGAP have since been documented in a wide variety of animal models and *in vitro* studies. A 15 amino acid peptide derivative, known as INGAP-P, encompassing the active center of INGAP has been identified, and shown to increase beta-cell mass and normalize glycemia in streptozotocin-induced diabetic mice [118]. Both INGAP-protein and INGAP-peptide were also shown to increase the number of insulin-positive cells, and overall insulin gene expression in healthy dogs following intramuscular injection [119].

The study of INGAP has reached phase II clinical trials, where 300mg or 600mg doses of 15aa INGAP-P were administered to a total of 63 T1DM patients and 126 T2DM patients using daily subcutaneous injections for a period of 90 days [120]. In the T1DM cohort, results demonstrated a significant increase in insulin C-peptide levels, as an indicator of increased insulin production, but a corresponding increase in glucose tolerance was not observed. These contradictory effects are thought to result from a parallel rate of autoimmune mediated islet destruction and de-novo islet formation, as evidenced by heightened GAD65 antibody titers [120]. For example, co-administration of INGAP and lisofylline, an anti-inflammatory agent, was found to significantly decrease diabetic symptoms in a Non-Obese Diabetic (NOD) mouse model, which by its very nature, possesses an autoimmune response against pancreatic closely resembling the pathophysiology of Type-1 diabetics [121]. In the T2DM cohort, a significant reduction in hemoglobin-A1C, an indication of mean blood glucose levels, was noted [120].

However INGAP-P presents a lower molar efficacy than INGAP protein throughout animal studies, even though both are known to act in a similar fashion, through the Ras-Raf-Erk pathway [122].

Recently both INGAP and INGAP-P were shown to induce the *in vitro* transdifferentiation of human pancreatic ductal epithelial cells into beta-like, insulin-positive cells, further supporting the theory of pancreatic ductal cell plasticity, and demonstrating the potency of INGAP [123]. A study by Madrid et al. has shown that INGAP can also increase insulin secretion and improve beta cell survival in mouse islets [124]. The benefits of INGAP may in fact extend beyond islet regeneration to improvements in peripheral nerve sensitivity, the loss of which is a common diabetic complication [125, 126]. Current INGAP research is primarily focused upon identifying the INGAP receptor, which is thought to be G-protein coupled (GPCR), and on elucidating its mechanism of action in beta cells, using ductal cells as in-vitro models [122, 127].

INGAP is a member of the Reg (short for regenerative) protein family, identified through analysis of a rat cDNA library in 1988 [128]. Members of this protein family are characterized by a C-type lectin carbohydrate binding domain, and divided into four subtypes [129]. Of note, Type I Regs are known to induce the proliferation of acinar and islet cells following secretion by the acinar cells in response to damage or pathological stress [130]. Type III Regs represent the largest category, notably encompassing RegIIIα, RegIIIβ, RegIIIγ, RegIIIδ, and INGAP [130-132]. These Regs are expressed throughout pancreatic tissue, but, aside from INGAP, are not significantly upregulated during the islet regeneration process, and are therefore believed to play a protective role, preventing apoptosis, as opposed to directly stimulating regeneration [130]. Type III Regs are also found to be expressed in various tissues of the gastro-intestinal tract such

as the duodenum and ileum, although their exact role in these contexts is still to be determined [130]. In contrast, INGAP is strongly expressed throughout islet regeneration, exclusively in pancreatic tissue, and is the only member of the Reg family with a demonstrated neogenic effect upon beta cells [133, 134].

## 1.8 MESENCHYMAL STEM CELLS (MSCS)

### 1.8.1 GENERAL PROPERTIES OF MSCS

Mesenchymal stem cells were initially identified in the bone marrow by Maureen Owen, due to their capacity for differentiation into cells of the mesodermal lineage, such as osteocytes, adipocytes lineages and chondrocytes, thereby serving as progenitors for these various connective tissues [135-137]. Isolation of MSCs is usually carried out using plastic adherence selection, where these cells will naturally adhere to tissue culture plates, allowing them to be segregated from other cell types in a tissue sample after a few passages [138]. The nomenclature “mesenchymal stem cell” has been the source of controversy in the scientific community, as many argue that the capability of these cells to differentiate into the aforementioned lineages does not necessarily constitute proof of “stemness”, instead of their identity being that of a progenitor [139]. For this reason, many publications refer to them as mesenchymal stromal cells [139]. However, the beneficial properties of MSCs in terms of regeneration, angiogenesis, immunomodulation, and ease of culture, as well as the promising results obtained in *in vitro*, *in vivo* and human clinical trials are undeniable [136, 140]

.

These cells all present numerous advantages as a vehicle for soluble gene product delivery. For example: genetically engineered MSCs expressing erythropoietin were shown to increase the hematocrit of mice with chronic renal failure, and retrovirally modified MSCs, implanted in a subcutaneous matrix in mice, slowed the proliferation of 4T1 breast cancer cells [141, 142]. MSCs also possess intrinsic "homing" properties, as defined by their ability to migrate specifically to sites of inflammation and tissue injury [143-145]. This action is not fully understood, but is believed to be partially mediated by CD44 and CD29 adhesion molecules allowing MSCs to traverse the vascular endothelium near the target organ when administered by intravenous injection [146]. Low levels of MSC migration have also been found following intraperitoneal injection [147]. In addition, MSCs participate in immunomodulation and tissue regeneration, through direct interactions with immune cells such as regulatory T cells, T-helper cells, inhibition of pro-inflammatory cytokines, and through the secretion of humoral factors which modify the local tissue microenvironment [148-151].

### 1.8.2 PREVIOUS USE OF MSCS IN DIABETIC RESEARCH

In accordance with the multipotent nature of MSCs, there is increasing evidence that MSCs possess the capacity to differentiate into fully functioning beta-cells [152]. Human bone marrow MSCs differentiated in the presence of various growth factors in glucose-rich medium for a period of 10 days acquired an expression profile similar to that of a mature beta cell, including transcription factors such as: PDX-1, Pax4, MafA, MafB, Ngn-3, NeuroD1 as well as the membrane GLUT-2 transporter, and the islet-specific enzymes PC1 and PC2 [153]. Injection of the resulting cell clusters into the renal capsule of nude diabetic mice provided full glycemic

control and elevated circulating levels of human insulin for a period of three months, whereas ablation of the treated kidney resulted in return to the diabetic state [153]. In contrast, while some MSCs injected in an undifferentiated state have been observed to acquire the ability to secrete insulin, this only occurred at an exceedingly low frequency, indicating that spontaneous in-situ differentiation under normal or diseased conditions are unlikely to occur [154].

Even though most of these cells may not differentiate while *in-vivo*, numerous studies have nevertheless demonstrated the benefits of injecting undifferentiated MSCs into diabetic animals and human patients, also attempting to elucidate the fate of these newly introduced MSCs [155]. Intrapancreatic injection of allogeneic bone-marrow MSCs into streptozotocin (STZ) induced diabetic mice produced significant improvements in glucose tolerance, insulin and C-peptide levels [156]. In a similar study performed in rats, MSCs were found to migrate from the injection site to the islets, where they would stimulate an increase in beta cell mass [154]. However, in other studies performed in the NOD mouse model, the observed benefits of MSC injections were shown to result from protective immunomodulatory effects during disease onset, rather than from regeneration [157]. The observed differences between experiments conducted in the NOD model and those conducted in the STZ model are likely due to the innate autoimmune response against islet antigens, as present in NOD mice, destroying beta cells as they are regenerated [155, 158]. The benefits of Mesenchymal Stem Cell injection could potentially be accentuated by combinatorial therapy, using a regenerative agent, to take full advantage of the respite afforded to beta cell populations by the reduced autoimmune response.

## 1.9 RATIONALE

Despite all therapeutic advancements, individuals affected by Diabetes Mellitus continue to suffer from severe complications and a significant reduction in life expectancy. Insulin therapy only serves to palliate the onset of these effects, and transplantation based therapies, while capable of restoring beta cell mass, are dependent on immunosuppressive therapies which render the patient highly vulnerable to other forms of disease. A curative therapy must therefore rely upon restoration of the native beta cell population. Since both INGAP and MSCs have been independently demonstrated to promote beta cell regeneration and an associated shift towards normoglycaemia, one could expect a more profound effect if they are used together. While simple co-injection may be envisaged for this purpose, a relatively short half-life of INGAP in serum (shown for INGAP-P) may limit the efficacy of this treatment [122]. Genetic engineering of the MSCs so that they continuously secrete INGAP when implanted in the patient would bypass the need for frequent injections. Additionally, several properties exhibited by MSCs could complement the actions of INGAP. The homing capabilities of these cells can allow for more efficient delivery of INGAP in or near the pancreas in the presence of inflammation, which MSCs may also help mitigate. Growth factors released by MSCs promote tissue vascularization and perfusion, which could provide support to a growing beta cell population [159]. Finally, MSCs have been safely used throughout a variety of human clinical trials, facilitating the translation of research findings from bench to bedside. To summarize: using MSCs for continuous *in vivo* INGAP delivery may result in synergistic effects, thereby improving islet regeneration and potentially providing a curative therapy for diabetes**.** This hypothesis is to be tested in a series of experiments, which will depend on the successful generation of INGAP-expressing MSCs. The latter is the main goal of the present study.

## 1.10 HYPOTHESIS

Mesenchymal Stem Cells (MSCs) can effectively express and secrete Islet Neogenesis-Associated Protein (INGAP) following gene transfer.

## 1.11 OBJECTIVE

The objective of this study is to demonstrate the capacity of MSCs to both produce and secrete INGAP following gene-modification.

## 1.12 SPECIFIC AIMS

1) Achieve transient transfection of bone marrow-derived mouse MSCs using a plasmid encoding INGAP cDNA.

2) Create an INGAP construct incorporating a C-terminal DDK (FLAG) tag for improved detection of recombinant INGAP.

3) Generate a viral plasmid encoding the optimized INGAP construct.

# CHAPTER 2: METHODS

## 2.1 BACTERIAL CULTURE

One-Shot™ DH5α E.coli (Thermo Fisher Scientific, MA, USA) were used for all subcloning experiments and for plasmid expansion and production. These cells were cultured using sterile LB Agar plates and LB Broth (Wisent, QC, Canada ) supplemented with either Ampicillin or Kanamycin, based on the specific selection requirements of the plasmid in question, attributed to their built-in resistance genes (Ampicillin selection for pcDNA 3.1D-V5-6His and AP2 plasmids, and Kanamycin selection for pCMV6). In order to minimize genetic variation, all cultures were streaked for isolation twice on LB agar plates (incubated overnight at 37°C), before individual colonies were picked and placed in 5ml liquid LB Broth culture for overnight expansion at 37°C. Miniprep and Maxiprep DNA extraction (Thermo Fisher) were carried out using 3ml and 250ml of liquid bacterial culture, respectively.

## 2.2 CELL CULTURE

### 2.2.1 COS-1 (AFRICAN GREEN MONKEY KIDNEY) CELLS

Culture and expansion was performed using DMEM F12 medium (ThermoFisher) supplemented with 10% FBS and 1% Penicillin/Streptomycin, which was changed every 2-3 days. Cells were passaged every 5 days, or when reaching approximately 90% confluency.

### 2.2.2 CHO (CHINESE HAMSTER OVARY) CELLS

Culture and expansion was performed in HAM's F12 medium (Thermo Fisher) supplemented with 10% FBS, 1% Penicillin/Streptomycin, and 1M L-Glutamine (Wisent), which was changed every 2-3 days. Cells were passaged every 5 days, or when reaching approximately 90% confluency.

### 2.2.3 MMSCS (MOUSE MESENCHYMAL STEM CELLS)

Cells were initially isolated from male C57BL/6 mouse femurs and tibias. The bodies of mice culled by cervical dislocation were rinsed in 70% ethanol, and their hindlimbs dissected to excise the bones. Using sterile technique in a biological safety cabinet, both ends of the femurs and tibias were cut, and a 25-gauge needle was used to flush out the marrow using complete culture media, consisting of MEM Alpha (1X) (Thermo Fisher) supplemented with 20% FBS and 1% Penicillin/Streptomycin. This marrow, suspended in culture media, was homogenated by five passages through a syringe fitted with an 18 gauge needle, before being cultured in T75 flasks at 37°C, 5% $CO_2$ (Thermo Fisher). Culture media was changed after the first 5 days, and then at 3 day intervals. Upon the observation of spindle-shaped colonies, cells were passaged into new flasks. At passage 8-9, flow cytometry was performed to determine the presence of CD44, CD73, CD90, CD105, and absence of CD31, CD45 surface markers, as is characteristic of MSC populations [160, 161]. All subsequent culture and expansion of purified cultures was performed in MEM Alpha (1X) (Thermo Fisher) supplemented with 10% FBS, 1% Penicillin/Streptomycin, and 1% L-Glutamine solution (200mM) (Wisent), which was changed

every 2-3 days. Cells were passaged every 6-7 days, or when reaching approximately 90% confluency. Only cells below passage #20 were used.

### 2.2.4 RINM5F (RAT INSULINOMA) CELLS

Culture and expansion was performed using RPMI 1640 medium (Thermo Fisher), supplemented with 2g/L sodium bicarbonate, 1% Penicillin/Streptomycin, 10mM HEPES (Thermo Fisher), and 1mM sodium pyruvate (Thermo Fisher). Cells were passaged every 5 days or when reaching approximately 90% confluency.

## 2.3 LIPOFECTAMINE (3000) TRANSFECTION

Cells were plated at 24 hours prior to transfection, in order to achieve approximately 90% confluency at the time of the experiment. Transfection was predominantly performed in 12-well culture dishes (Thermo Fisher) with 3.8$cm^2$ of surface area per well. For transfection experiments performed in other cultureware, reagent volume was adjusted based on relative surface area. See Table 1 for the optimized transfection reagent volumes for each cell type, in a 12-well culture dish. One hour before transfection, culture media was aspirated, cells were washed once with PBS (1X), and serum-free Opti-MEM media was added to the wells (Thermo Fisher). Approximately 15 minutes before the start of the experiment the plasmids encoding INGAP cDNA were thawed on ice, and lipofectamine 3000 and P3000 booster reagents were vortexed gently and placed at room temperature. For each transfection reaction, two tubes were prepared : One containing Opti-MEM and a pre-determined volume of lipofectamine, and the

other containing Opti-MEM, and pre-determined amounts of DNA and P3000 booster. Once prepared, these mixes were incubated for five minutes at room temperature, before being combined and incubated for a further five minutes at room temperature. The entirety of the resulting solution was then gently pipetted into the culture wells. Plates were rocked from side to side to insure proper distribution of the reagents. Swirling was avoided. Cells were incubated for 24-48 hours in the presence of the transfection reagents before being used for further experimentation. Transfection efficacy was evaluated by Western Blot and Immunocytochemistry.

**Table 1** Optimized Transfection Reagent Volumes per Cell Type in a 12-well Culture Dish (surface area of 3.8cm$^2$/well)

| **Cell Type** | **mMSC** | **CHO** | **Cos-1** |
|---|---|---|---|
| **Plasmid DNA (ug)** | **2** | **2** | **2** |
| **Lipofectamine 3000 (ul)** | **4.8** | **3.8** | **3** |
| **P3000 Booster (ul)** | **4** | **4** | **4** |

## 2.4 IMMUNOCYTOCHEMISTRY

All immunofluorescence experiments were performed in 8-well chamber slides (Sarstedt, Germany). Cells were transfected using lipofectamine 3000, as previously described, and fixed for 10 minutes using either 100µl/well of 4% formalin; or 100µl/well of 100% pre-chilled methanol at -20°C, followed by drying at ambient temperature. The wells were then blocked for

30mins with 5% donkey serum in PBS, followed by three washes with PBS. Probing was carried out using either mouse-anti-6His (1:500 dilution, Thermo Fisher) or rabbit-anti-INGAP (1:400 dilution, custom made by GenScript, China) primary antibodies, and their respective donkey-anti-mouse CY3 conjugated (1:2000 dilution) and donkey-anti-rabbit Alexa Fluor 488 conjugated (1:2000 dilution) secondary antibodies, diluted in 1% donkey serum in PBS. Three washes in PBS were performed after the incubation of each antibody. After removing the plastic well chambers from the slide, coverslips were mounted using Vectashield® Hardset™ mounting medium with DAPI nuclear stain (Vector Laboratories, CA, USA), and imaged using an Olympus® Fluoview™ FV10i confocal microscope (Olympus, Japan).

## 2.5 CELL LYSIS AND PREPARATION OF LYSATES

Cell lysis buffer was prepared from 10X lysis buffer concentrate (Cell Signaling, MA, USA), by diluting 1:10 with double distilled water, and adding one EDTA-free protease inhibitor tablet (Thermo Fisher). Cell culture plates were washed with PBS and placed on ice, after which the lysis buffer was added: 120µl for 6-well plates, 50µl for 12-well plates, and incubated for 5 minutes. Rubberized cell scrapers (Sarstedt) were then used to agitate and pool the lysate, which was collected into 1.5ml tubes (Corning, NY, USA) and immediately placed on ice. These samples were then sonicated, each for 10 seconds, using a 4710 Ultrasonic Homogenator (Cole-Parmer, IL, USA), and centrifuged for 10 minutes at 14000g in a table-top mini-centrifuge at 4°C. Lysates were subjected to assay of total protein content to establish loading amounts. This was carried out in a 96 well tissue-culture plate (Thermo Fisher), where 3 repeats (5µl each) of each lysate sample were pipetted into their respective wells, to which 25µl/well of DC-Protein

Assay Reagent A was added (Containing 20 µl/ml of DC-Protein Assay Reagent S), along with 250µl/well of DC-Protein Assay Reagent B (BioRad, CA, USA). Serial dilutions of Bovine Serum Albumin (BSA) were also loaded in separate wells to establish a standard curve. After a 5 minute incubation period, the 96-well plate was analyzed using a Benchmark™ microplate reader (Bio-Rad). Once approximate total protein concentrations were established, 25µg of each sample was mixed with 4X Laemmli Sample Buffer containing 10% β-Mercapto-ethanol at a ratio of 3:1 (Bio-Rad). The lysates were then heat-shocked for 5 minutes at 95°C and then cooled on ice in preparation for Western Blot analysis.

## 2.6 WESTERN BLOT

Western blot was utilized to verify the presence of INGAP, both in cell lysates and 48h conditioned media, as well as to provide approximations of INGAP concentration in conditioned media. Samples (25µg protein) were resolved on 12.5% SDS-PAGE gel, at 100V for 75 minutes followed by overnight transfer to a 0.2µm nitrocellulose membrane (Bio-Rad) at 35V. Membrane were blocked 30 minutes using 5% milk in tris-buffered saline supplemented with Tween 20 (TBST). Probing was performed using one of three primary antibodies : INGAP-specific (custom made, GenScript), 6-His-specific (Thermo Fisher), and DDK-specific (Thermo Fisher), and an anti-rabbit or anti-mouse HRP-conjugated secondary antibody. All of these antibodies were diluted in 10ml-12ml of 5% Milk in TBST. Several washes in TBST were performed between each step of this procedure. Membranes were developed with Clarity™ ECL Western Blot Detection Reagents (BioRad) and imaged on a Chemidoc-MP™ fluorescence and chemiluminescence imager (BioRad).

## 2.7 POLYMERASE CHAIN REACTION (PCR) AMPLIFICATION

PCR amplification was utilized to verify the ligation of INGAP cDNA within the plasmids under study. This procedure was necessary for the AP2-INGAP-DDK plasmid, instead of the more commonly used restriction digestion method, due to deletion of the vector's 3' restriction site by the blunting step used during sub-cloning. Each reaction sample contained: 4µl PCR Pure water, 5µl of a primer mix containing 1µm of 5' INGAP forward primer (Fig.1) and 1µm of 3' INGAP reverse primer (Fig.1), 10µl iQ™ CYBR® Green (BioRad), and 1ng of DNA from the target plasmid. Amplification was carried out for 25-40 cycles using a C1000™ Thermal Cycler/CFX9™ Real-Time System (BioRad). Presence of INGAP cDNA was assessed based on Cq values and melting temperature in comparison to a negative control loaded with water (no plasmid DNA) and to positive controls consisting of plasmid DNA known to contain INGAP. Amplicons were verified by DNA electrophoresis on a 1% agarose gel.

**Figure 1** INGAP-Specific Primer Sequences used for qPCR Analysis and Sequencing of New Constructs.

**Forward**: TGGGTGGAAGGTGAAGAATCTC (Corresponds to 102-123bp on INGAP cDNA).

**Reverse**: CAATAACCACGGTCAGCAGCAA (corresponds to 472-451bp on INGAP cDNA).

**Amplicon size**: 370bp

Based on full INGAP sequence as published by Rafaeloff et al [117].

## 2.8 ASSAY OF INGAP ACTIVITY

To assay the activity of DDK tagged INGAP protein, its concentration in conditioned media harvested from transfected Chinese Hamster Ovary (CHO) cells had to be estimated to provide a low-nanomolar range of concentration for the treatment of target cells (RINm5F). This was performed through the comparison of 5ul, 10ul, and 24ul of comditioned media to a standard curve of purified 6His tagged recombinant INGAP, of known concentration, by Western Blot analysis. Quantification of the observed signal intensity was performed using Image Lab™ software (BioRad). Rat insulinoma (RINm5F) cells, an in-vitro model of the pancreatic beta cell, were cultured to approximately 80% confluency in 35mm culture plates (Thermo Fisher), and switched to serum-free RPMI 1640 culture medium (Thermo Fisher) 24 hours before experimentation. Approximate 1nM and 5nM concentrations of INGAP-DDK were then utilized to treat the RINm5F cells for a period of exactly 10 minutes, followed by cell lysis and the collection of lysates as per the method listed in section 2.5. This procedure was also performed with 1nM and 5nM concentrations of purified 6His tagged rINGAP, as a positive control, and with comparable volumes of conditioned media harvested from untransfected CHO cells, and from CHO cells transfected with empty pCMV6 vector, serving as negative controls. An additional negative control consisted of untreated Rinm5F cells. The upregulation of Erk 1/2 phosphorylation in response to INGAP treatment, a known indicator of INGAP activity, was determined by Western Blot of these Rinm5F cell lysates using a rabbit-anti-P-p44/42 MAPK primary antibody to detect phospho-Erk 1/2, and a rabbit-anti-p44/42 MAPK primary antibody to detect total Erk 1/2 (New England Biolabs, MA, USA), along with their corresponding HRP-conjugated goat-anti-rabbit secondary antibodies. Quantification of signal intensity (band volume) was once again carried out using Image Lab™ software (BioRad). Finally, Phospho-Erk

1/2 upregulation was calculated using the ratio of band volume from detected phospho-Erk 1/2 over that of detected total Erk 1/2. These ratios were normalized to that of the negative control consisting of untreated cells, probed on the same blot. Results from different replicates and experiments were averaged.

## 2.9 SUB-CLONING OF INGAP CDNA

For each successive plasmid modification: 3-10μg samples of the starting vector and destination vector were subjected to overnight digestions using the appropriate restriction enzymes (Hind III, EcoRV, Bgl II, Pme I, BamH I, from New England Biolabs). Preparation of the AP2 vector DNA required blunting using Mung Bean Nuclease (New England Biolabs). Samples requiring multiple digestion steps in different buffers were purified between each buffer change using the Monarch™ DNA purification kit (New England Biolabs). Once digested, all samples were then run for 1 hour at 100 volts on a 0.8%-1% D1-LE low-melt agarose gel (VWR, PA, USA). Presence of digestion products was validated and recorded using a BioRad *ChemiDoc MP*™ imaging system.

Using a UV trans-illuminator to visualize the digested DNA. The desired vector and insert bands were then cut out of the gel using a razor blade, weighed, and solubilized in 3 volumes of QG buffer (Thermo Fisher). The Quiagen Gel Extraction kit (Thermo Fisher) protocol was then followed to obtain purified DNA. The final elution step was carried out using DEPC-treated water instead of the supplied elution buffer. In the event of low DNA concentration following extraction, samples were concentrated using a Savant™ SC110A SpeedVac®-Plus concentrator (Thermo Fisher).

Overnight ligation of 0.3µg purified vector and 0.22µg insert DNA was performed using 3µl T4 ligase and 6µl ligation buffer (New England Biolabs) in a total volume of 20µl at room temperature. The reaction was stopped by heat inactivation for 10 minutes at 65°C followed by a 5 minute chilling on ice. The ligation product, along with a pUC19 control plasmid (Thermo Fisher) were then used for E.coli DH5α transformation. 50µl of One-Shot™ DH5α competent cells (Thermo Fisher) were exposed to 5µl of ligation product or pUC19 for 30 minutes on ice. A 30 second heat shock at 42°C was performed followed by immediate cooling on ice. 250µl of warm SOC medium was then added to the cells, which were incubated for 1hour at 37°C/200 rpm in a temperature-controled orbital shaker. Two aliquot sizes (20µl and 200µl) were spread on LB agar plates containing 25µg/ml of the appropriate selection antibiotic and incubated overnight at 37°C.

Colonies obtained were picked and streaked for isolation on a second LB plate, before being grown in 5ml of LB broth + Antibiotic overnight. Plasmid DNA was isolated from these cultures as per the Quiaprep Spin Miniprep Kit or Quiaprep Maxiprep Kit protocol (Thermo Fisher). The final elution step was carried out with DEPC-treated water instead of the supplied elution buffer. The overall success of the subcloning procedure was confirmed by endonuclease digestion, to excise the INGAP cDNA, visualized on a 1% agarose gel and/or by PCR amplification.

# CHAPTER 3: RESULTS

## 3.1 VALIDATION OF STARTING CONSTRUCT : PCDNA 3.1D-V5-6HIS-INGAP

pcDNA 3.1D-V5-6His-INGAP, generated throughout previous studies, was utilized as the starting plasmid to develop all subsequent INGAP constructs seen in this study. There exists two variants of this plasmid: one bearing 6-His tagged INGAP, known as the (3-6) construct; and one bearing both INGAP-linked 6-His and V5 tags, known as the (1-1) construct (Fig. 2A). To test the integrity of these starting INGAP constructs, plasmid DNA was extracted from bacterial cultures, and subjected to overnight endonuclease restriction digestion and DNA electrophoresis (Fig. 2B). Presence of INGAP cDNA was confirmed through comparison between the size of digested fragments and expected sizes, based on the full INGAP sequence [117]. Linearization using Xba1 enzyme produces a band representing the entire expected plasmid size : 6043bp for pcDNA 3.1D-V5-6His 1-1, and 6066bp for pcDNA 3.1D-V5-6His 3-6. Double digestion using Xba1 and Kpn1 excises the INGAP cDNA from the vector, producing large bands in the 5500bp range which correspond to the vector's 5443bp, and fainter bands in the 600bp range corresponding respectively to the 602bp and 623bp sizes of the 1-1 and 3-6 construct variants. In this case, the size difference between both variants is clearly visible, with the 1-1 DNA running slightly higher than the 3-6 DNA. Finally, endonuclease digestion using BstX1 was used to cut the vector at two sites, one near the center of the INGAP construct, and one in close proximity, downstream of INGAP, thereby producing two fragments of approximately 5600bp and 400bp as expected. The smaller ~400bp fragment could not have been present if INGAP was absent from the construct, through lack of a second cleavage site.

**Figure 2** Restriction Digestion of pcDNA 3.1D-V5-6His-INGAP. Starting plasmid maps ("1-1" and "3-6" constructs) (**A**). Electrophoresis results from the digestion of both starting plasmids displaying the correct fragment sizes for each respective digestion (**B**).

**A**

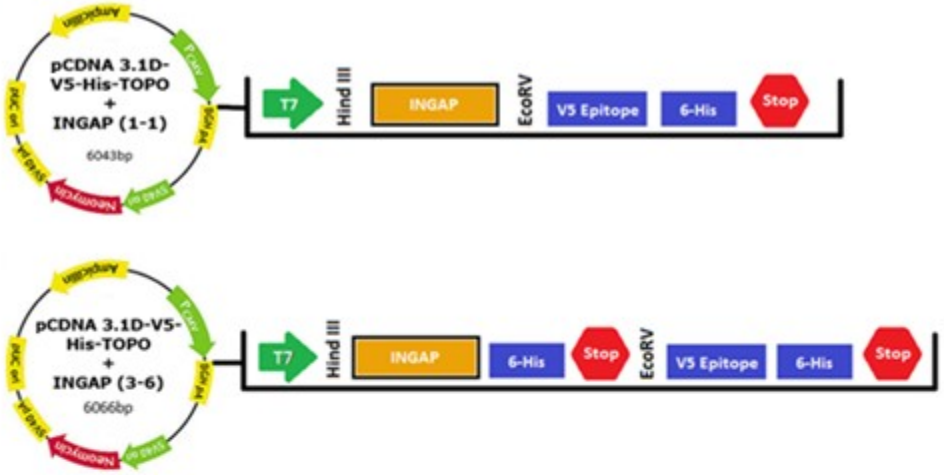


**B**

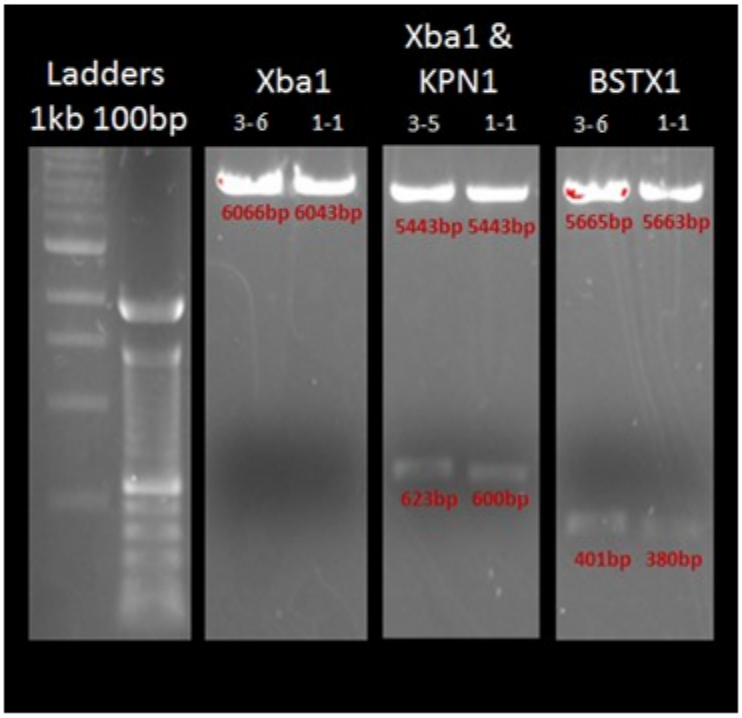

## 3.2 TRANSIENT LIPOFECTION OF IMMORTALIZED CELL LINES

In order to demonstrate the ability of mammalian cells to both produce and secrete INGAP, and the capacity of the pcDNA 3.1D-V5-6His vector to introduce INGAP cDNA into these cells under transfection conditions, two immortalized cell lines frequently used in laboratory settings, SV40 transformed african green monkey kidney cells (Cos-1) and Chinese Hamster Ovary (CHO) cells were subjected to 48hour transfection using lipofectamine 3000 and the pcDNA 3.1D-V5-6His vector. The lysates of Cos-1 were assayed by Western Blot (Fig.3). Both lysates and conditioned media from transfected CHO cells were collected and assayed by Western Blot (Fig.4). The presence of INGAP was clearly identifiable in all cases, based on the 17.6 kDA molecular weight of the 6-His tagged "3-6" variant (Fig. 3-lane 6 & 7, Fig. 4A-lane 3 to 6, Fig. 4B-lane 3 & 4), of the same size as purified recombinant INGAP (lane 1 in Fig. 3 & 4), and on that of the larger 21.9kDa "1-1" construct bearing both 6-His and V5 tags (Fig. 3-lane 6 &7, Fig. 4-lane 7 to 10, Fig. 5-lane 5 & 6). A large non-specific band was present in all lysate samples (Fig. 3 & 4A), at a size intermediate to the two pcDNA 3.1D-V5-6His variants, but only faintly observed in conditioned media (Fig. 4B). A variety of experimental conditions, based on the overall lipofectamine concentration and duration of cellular exposure to the reagents, were assayed in order to optimize the transfection procedure. An exposure time of 48 hours to transfection reagents in Opti-Mem medium (ThermoFisher Scientific, MA, USA) was found to be efficient in all tested cell lines. See table 1 for optimized tranfection reagent volumes in a 12-well culture dish.

**Figure 3** Expression of INGAP in Transiently Transfected Cos-1 cells. Western Blot analysis of cell lysates after 48h lipofectamine transfection.

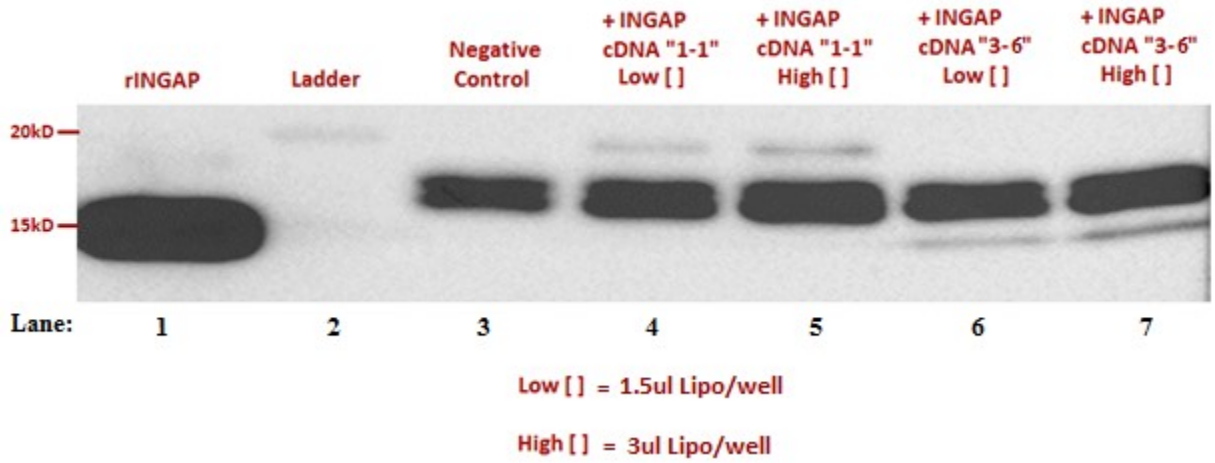

**Figure 4** Expression and secretion of INGAP in Transiently Transfected CHO cells. Western Blot of lysates (**A**) and conditioned media (**B**) harvested from cells transfected for 24h & 48h using Lipofectamine 3000.

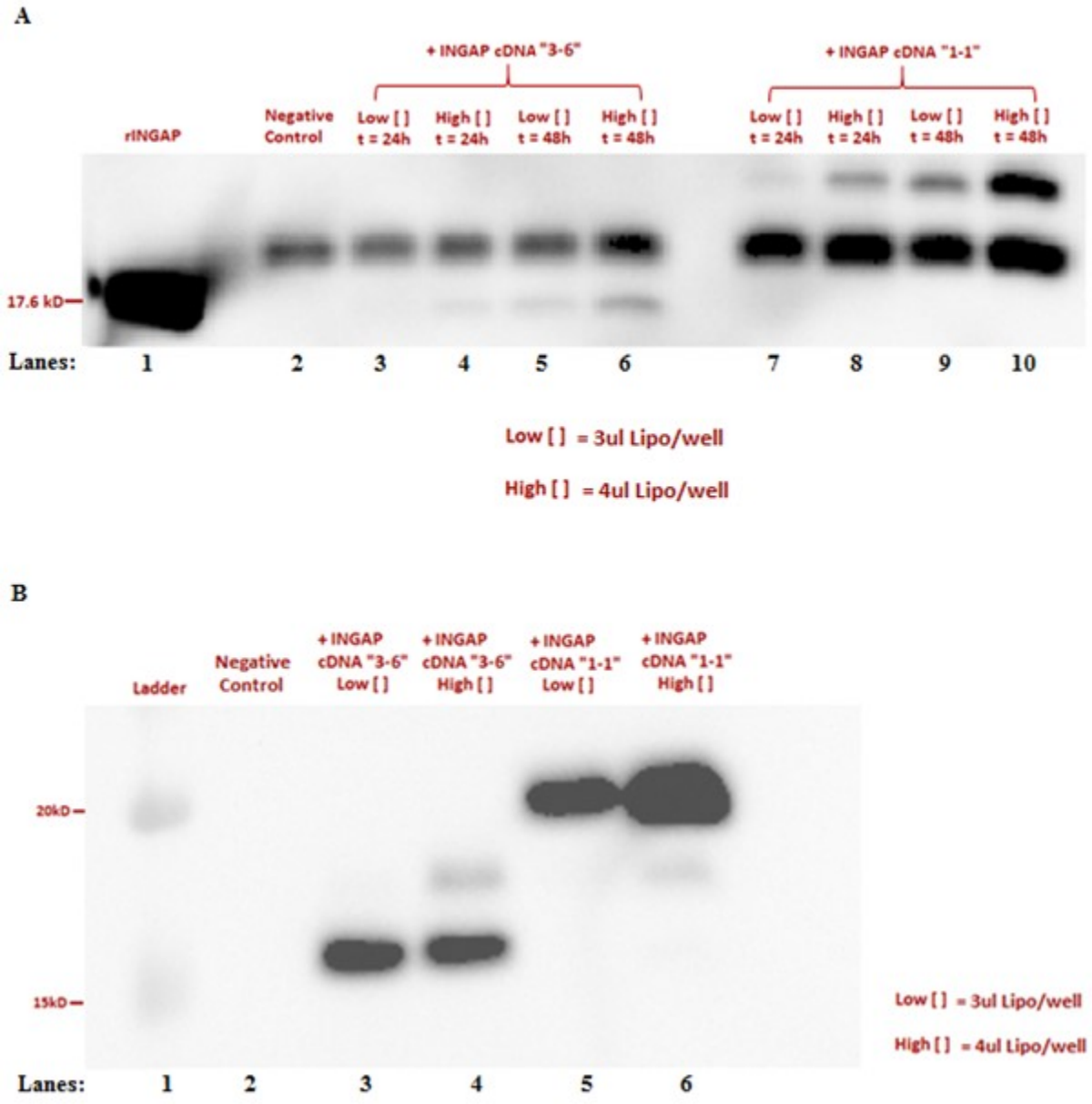

## 3.3 TRANSIENT LIPOFECTION OF PRIMARY MOUSE MESENCHYMAL STEM CELLS (MSCS).

Mouse bone-marrow MSCs expressing INGAP were generated following 24-72hr liposomal transfection using pcDNA 3.1D-V5-6His plasmids encoding the full length INGAP protein. As demonstrated in figure 5, the production and secretion of mature INGAP was demonstrated via Western Blot, probed using a rabbit-anti-INGAP specific primary antibody, followed by HRP conjugated goat-α-rabbit secondary antibody (Fig. 5D). Confocal fluorescence microscopy was further used to confirm the cytoplasmic localization of the protein, using both mouse-anti-6-his (Fig. 5A) and rabbit-anti-INGAP (Fig. 5B & C) primary antibodies, and their respective donkey-anti-mouse CY3 linked and donkey-anti-rabbit alexa-fluor-488 linked secondary antibodies. Cell nuclei were counterstained using DAPI (in blue). Unfortunately, due to high variability between immunofluorescence results, a definitive rate of transfection efficacy could not be established, and is likely lower than 10% based on qualitative observations.

**Figure 5** Expression of INGAP (6-His-tagged) in Transiently Transfected Mouse MSCs. Detection of immunofluorescence by confocal microscopy in MSCs probed with anti-6His primary/CY3-linked secondary antibody (**A**) and anti-INGAP primary/AlexaFluor 488-linked secondary (**B & C**). Detection of secreted INGAP by Western Blot with anti-INGAP antibody (**D**).

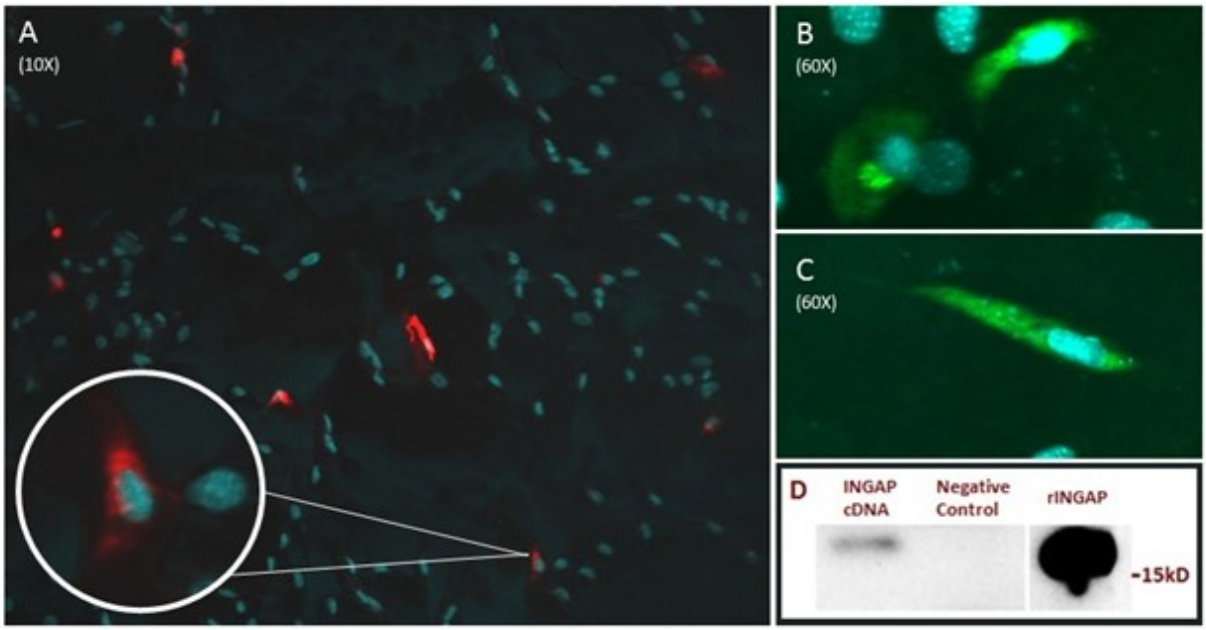

## 3.4 DESIGN OF IMPROVED INGAP CONSTRUCTS (DDK-TAGGED)

Two new constructs, designed for more efficient INGAP delivery and enhanced protein detection, were produced through sub-cloning using HindIII and EcoRV endonucleases. INGAP cDNA was transferred from pcDNA 3.1D-V5-6His to pCMV6 (OriGene, MD, USA), where it was linked to this new plasmid's inherent DDK tag. This newly modified plasmid is referred to as: pCMV6-INGAP-DDK, and features DDK tagged INGAP expressed via a CMV promoter, as well as Kanamycin antibiotic resistance. The Myc tag, present in the original pCMV6 has effectively been eliminated by the restriction digestion process, leaving only the desired DDK tag (Fig. 6). For use as a control in future experiments, a second plasmid was conceived, reffered to as pCMV6-INGAP-6His, using INGAP-6-His cDNA at the same position within pCMV6, but retaining a stop codon between the 6-His tag and the plasmid's DDK tag (Fig. 7). The efficiency of digestion, to prepare the pCMV6 vector and INGAP insert fragments, was confirmed by DNA electrophoresis (Fig. 8), as was the final plasmid size and successful incorporation of INGAP and INGAP-6His cDNA into pCMV6 (Fig. 9A, Fig. 9B). Samples of pCMV6-INGAP-DDK, along with INGAP-specific primers (Fig. 1), were sent to the McGill University Genome Center/Genome Quebec for Sanger sequencing to confirm insertion of INGAP cDNA in the correct orientation, and linkage to the DDK tag (Fig. 10).

**Figure 6** Construct Design Workflow and Restriction Site Overview : pCMV6 – INGAP-DDK

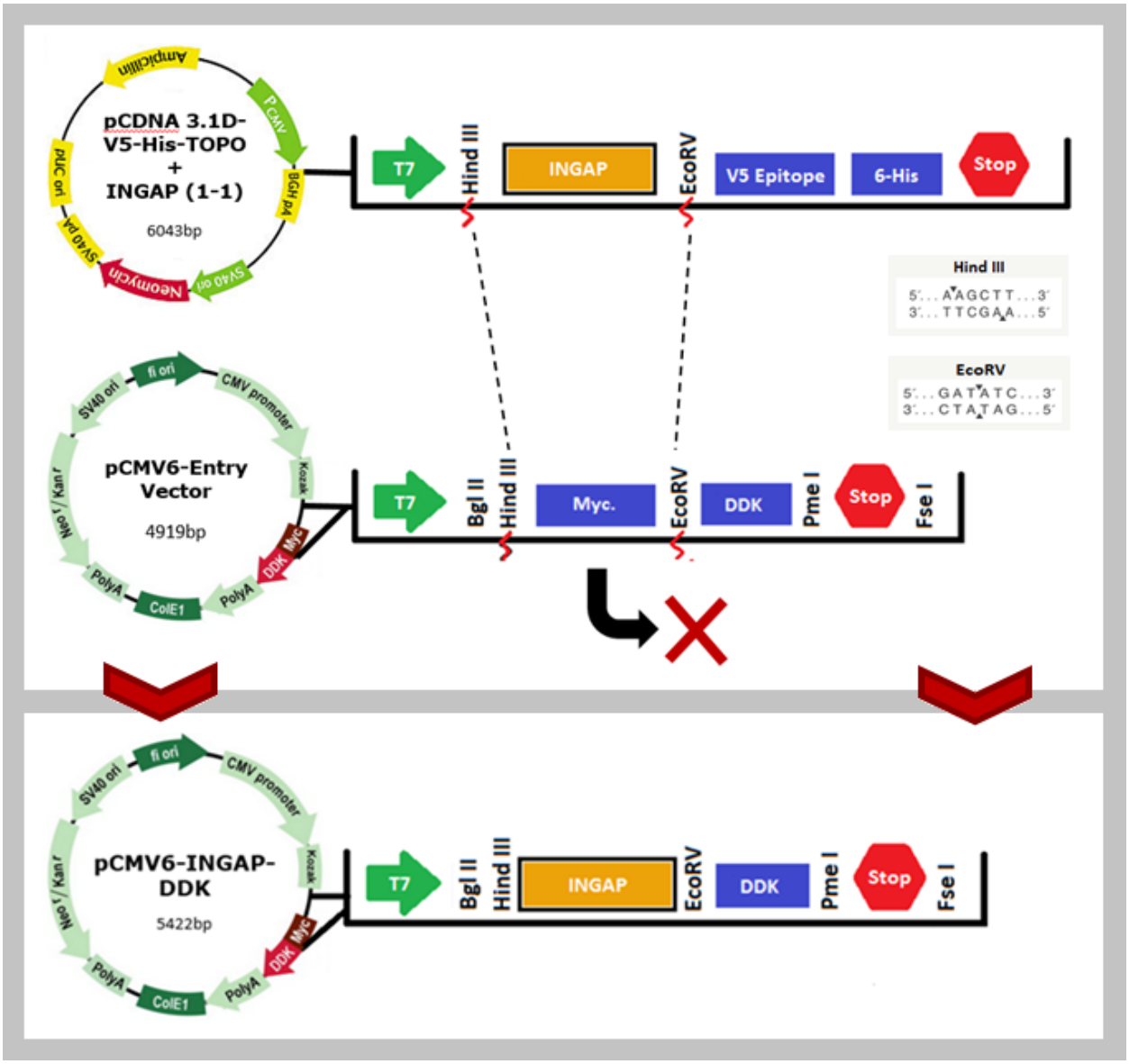

**Figure 7** Construct Design Workflow and Restriction Site Overview : pCMV6-INGAP-6His

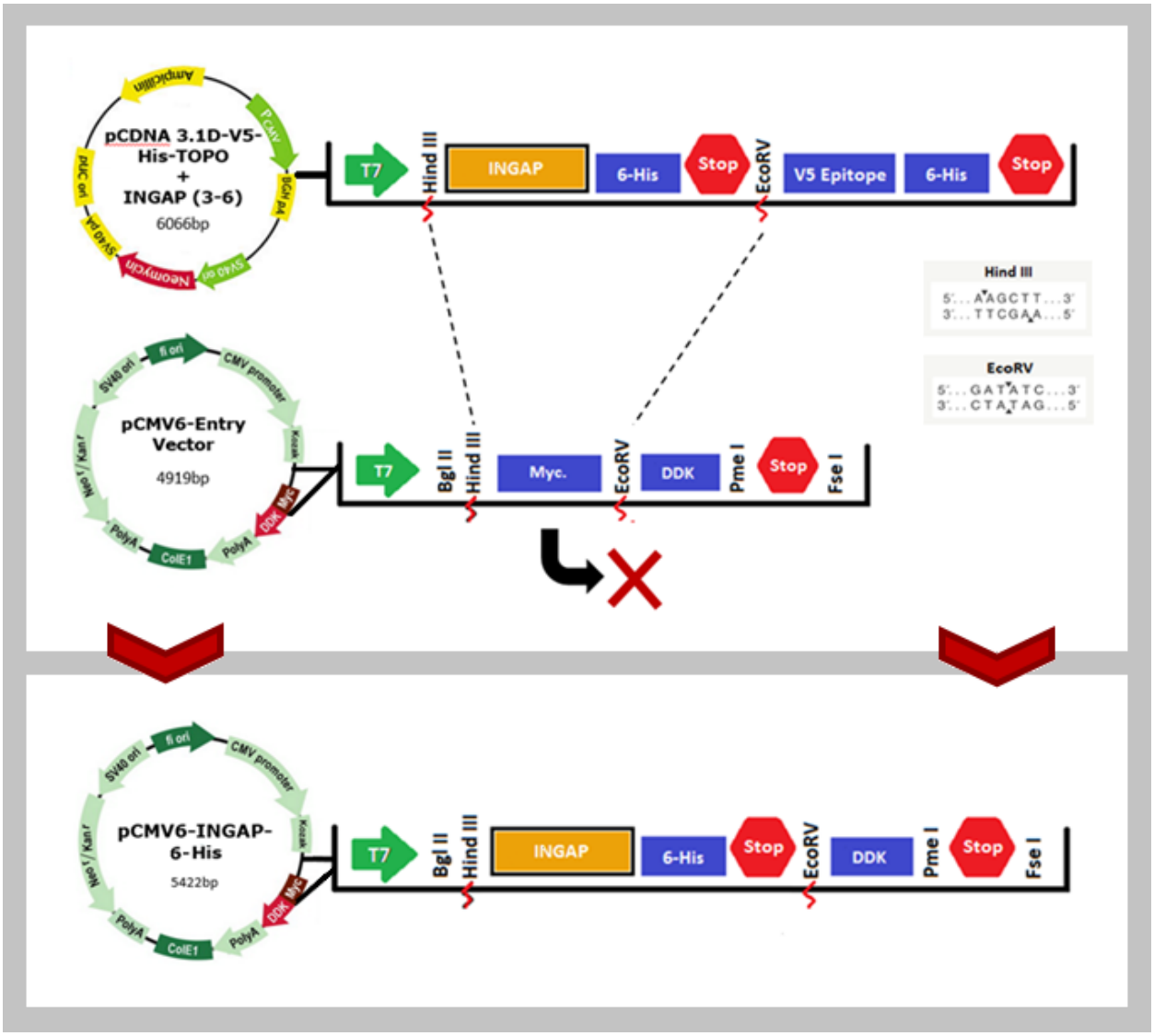

**Figure 8** Restriction Digestion of pCMV6 and pCDNA 3.1D-V5-6His-INGAP using Hind III and EcoRV to Produce Ligation-ready DNA.

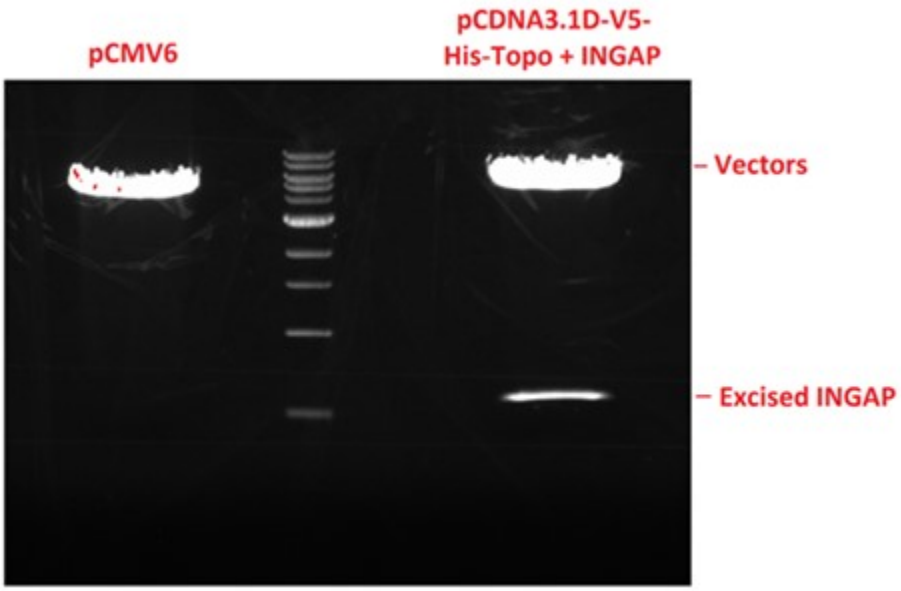

**Figure 9** Restriction digestion of pCMV6-INGAP-DDK (**A**) and pCMV6-INGAP-6His (**B**). Successful ligation of INGAP and INGAP-6His into pCMV6 confirmed by excision of the original inserts.

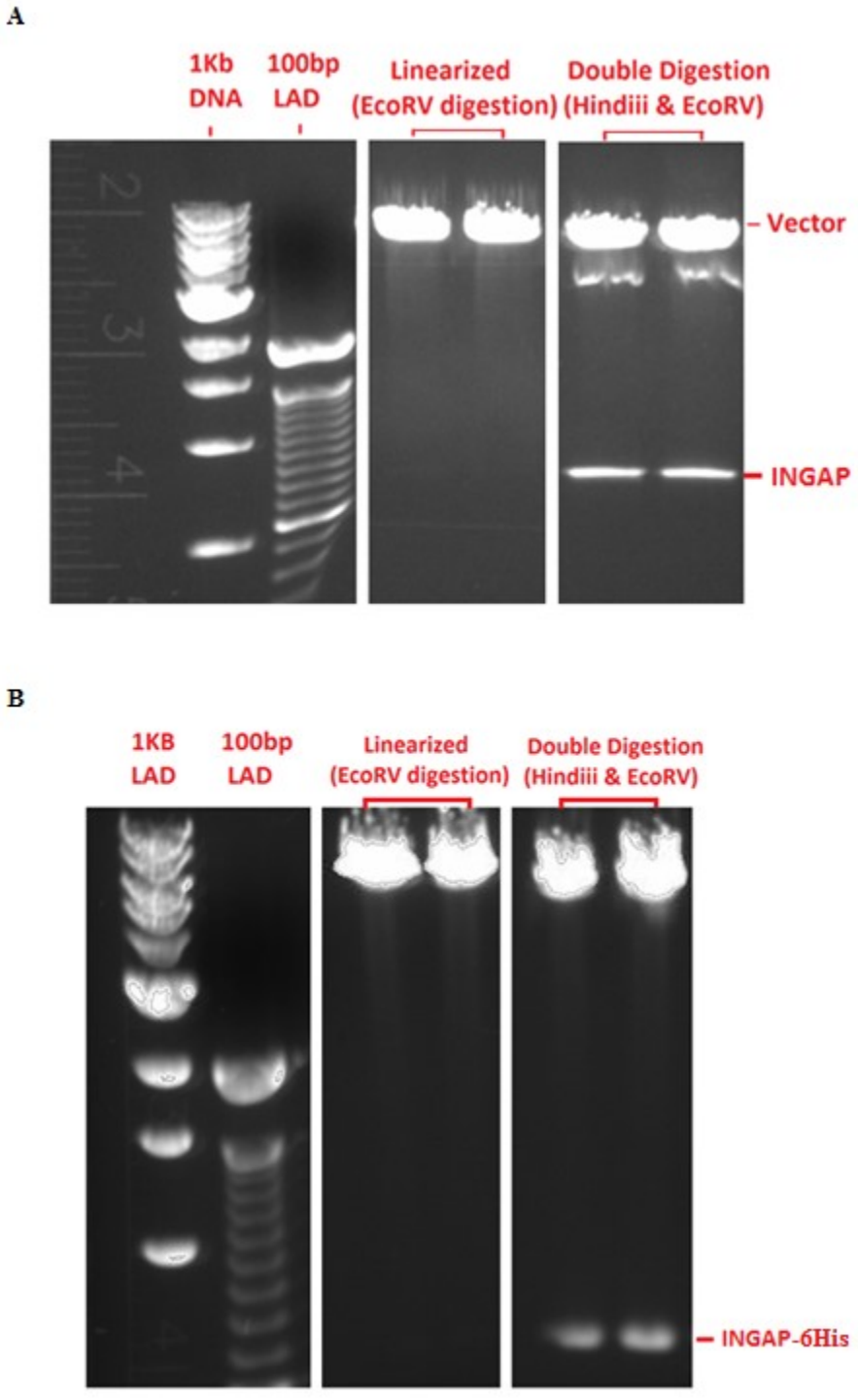

**Figure 10** Results of Sanger Sequencing for the pCMV6-INGAP-DDK plasmid.

**Legend:**

-Correct INGAP
-DDK Tag
-pCMV6 Vector

cttggcagtacatctacgtattagtcatcgctattaccatggtgatgcggttttggcagtacaccaatgg
gcgtggatagcggtttgactcacggggatttccaagtctccaccccattgacgtcaatgggagtttgttt
tggcaccaaaatcaacgggactttccaaaatgtcgtaataaccccgccccgttgacgcaaatgggcggta
ggcgtgtacggtgggaggtctatataagcagagctcgtttagtgaaccgtcagaattttgtaatacgact
cactatagggcggccgggaattcgtcgactggatccggtaccgaggagatctgccgccgcgatcgccggc
gcgccagatctcaagcttggtaccgagctcggatccagtaccttcaccatgatgcttcccatgaccctc
tgtaggatgtcttggatgctgctttcctgcctgatgttccttttcttgggtggaaggtgaagaatctcaaa
agaaactgccttcttcacgtataacctgtcctcaaggctctgtagcctatgggtcctattgctattcact
gattttgataccacagacctggtctaatgcagaactatcctgccagatgcatttctcaggacacctggca
tttcttctcagtactggtgaaattaccttcgtgtcctcccttgtgaagaacagtttgacggcctaccagt
acatctggattggactccatgatccctcacatggtacactacccaacggaagtggatggaagtggagcag
ttccaatgtgctgaccttctataactgggagaggaaccccctctattgctgctgaccgtggttattgtgca
gttttgtctcagaaatcaggttttcagaagtggagagattttaattgtgaaaatgagcttccctatatct
gcaaattcaaggtcaagggtcaagacaattctgcagatatcctggattacaaggatgacgacgataaggt
ttaaacggccggccgcggtcatagctgtttcctgaacagatcccgggtggcatccctgtgacccctcccc
agtgcctctcctggccctggaagttgccactccagtgcccaccagccttgtcctaataaaattaagttgc

**Translated sequence**

MMLPMTLCRMSWMLLSCLMFLSWVEGEESQKKLPSSRITCPQGSVAYGSYCYSLILI
PQTWSNAELSCQMHFSGHLAFLLSTGEITFVSSLVKNSLTAYQYIWIGLHDPSHGTL
PNGSGWKWSSSNVLTFYNWERNPSIAADRGYCAVLSQKSGFQKWRDFNCENELPYIC
KFKVKGQDNSADILDYKDDDDKV

**Expected mw: 18.9kD**

## 3.5 CONFIRMATION OF INGAP-DDK EXPRESSION AND SECRETION

The capacity of the newly generated pCMV6-INGAP-DDK to induce production and secretion of INGAP in mammalian cells was assayed through transient lipofection of this plasmid into CHO cells. Lysates collected from these transfected cells was assayed by Western Blot (Fig.11). Probing was first performed using mouse-anti-DDK specific primary and goat-anti-mouse HRP conjugate secondary antibodies (Fig. 11A). Two clear demarcations, indicating the presence of INGAP-DDK, can be found at the correct molecular weight of approximately 18.9 kDA in all lysates from cells transfected with pCMV6-INGAP-DDK (Lanes 3 & 4). No band of this molecular weight is visible in the lanes corresponding to the negative control: untransfected cell lysate (Lane 5). This same Western Blot membrane was also stripped and re-probed using rabbit-anti-INGAP primary antibody followed by goat-anti-rabbit secondary antibody, which produced corresponding results: a strong INGAP signal is present in media from transfected cells (Fig. 11B, Lanes 3 & 4). A faint non-specific band of the same molecular weight seems to be present in all control lanes. The presence of INGAP is also noted in both positive controls: 17.6kD recombinant INGAP (Lane 1), and the original pcDNA 3.1D-V5-6His (1-1) plasmid (Lane 7). The visible bands in these controls are of different size to those of INGAP-DDK, as expected based on the variations in protein size resulting from the different tags in each version of INGAP. The secretion of INGAP-DDK from CHO cells was then assayed by Western Blot of conditioned media from the same transfection experiment (Fig.12). Strong signals are present for both INGAP-DDK (Lane 13 & 14) and INGAP-6His (Lane 11 & 12), as well as the recombinant INGAP positive control. No signal is observed in the lane corresponding to the negative control: conditioned media from untransfected cells.

**Figure 11** Expression of INGAP-DDK in Transiently Transfected CHO Cells. Western Blot of lysates probed with anti-DDK antibody (**A**) and anti-INGAP antibody (**B**).

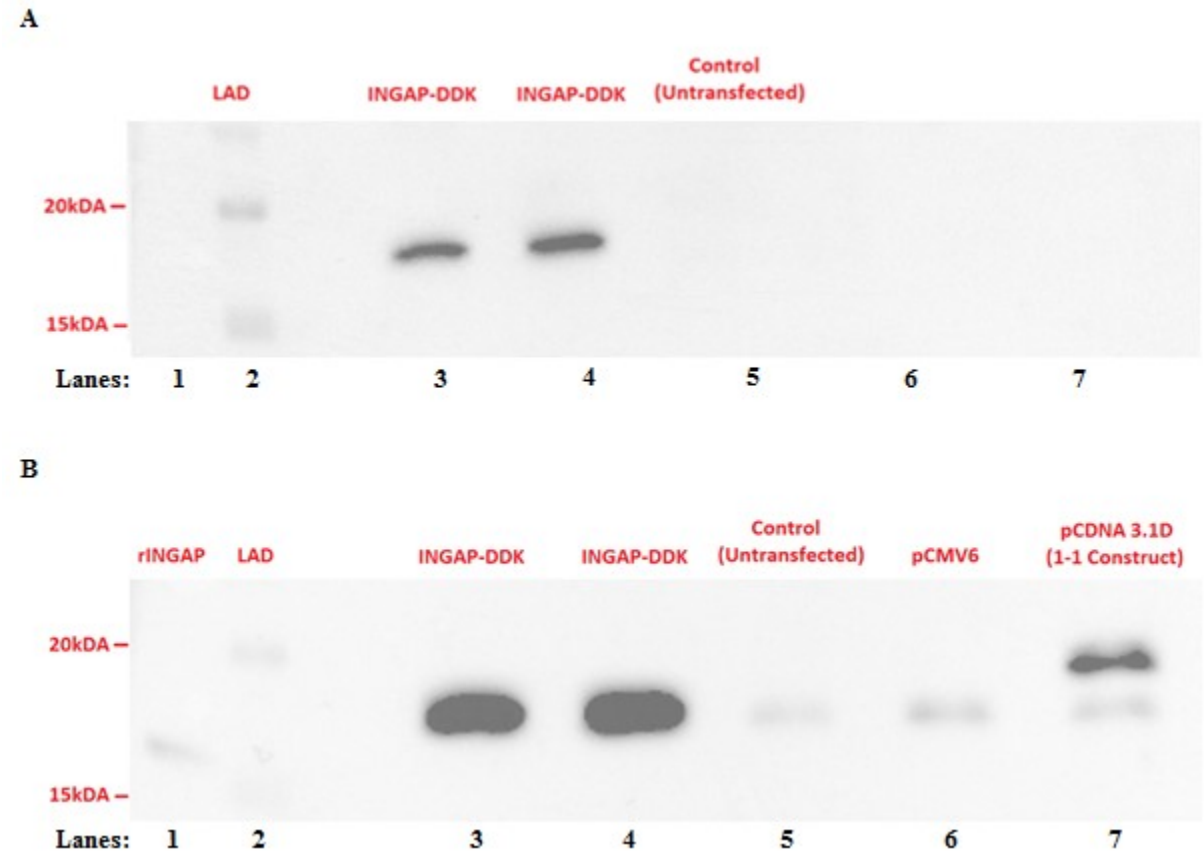

**Figure 12** Expression and Secretion of INGAP-DDK in Transiently Transfected CHO Cells. Western Blot of conditioned medium probed with anti-INGAP antibody.

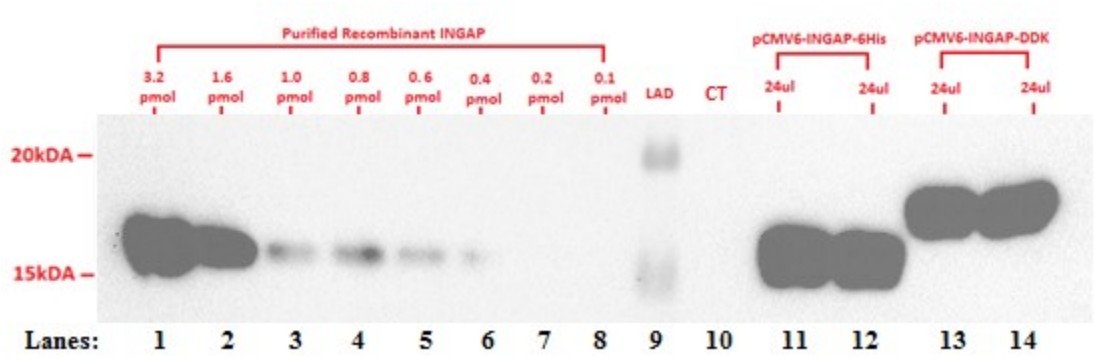


## 3.6 ASSAY OF INGAP-DDK ACTIVITY

The activity of INGAP-DDK was assessed by its capacity to induce Erk 1/2 phosphorylation in RIN-m5F cells after 10 minutes of exposure, as previously described for rINGAP [122]. Since this effect was shown to be dose-dependant (optimal at 1nM), it was important to administer INGAP-DDK at a similar concentration. An approximate quantification of secreted INGAP-DDK was performed by Western Blot analysis of incremental volumes of conditioned media from transfected CHO cells (5µl, 10µl, 24µl), probed with anti-INGAP primary/anti-rabbit secondary antibody (Fig.13, Lanes 12 to 14). Band volumes, quantified using Image Lab™ software (BioRad, CA, USA), were compared to those of a standard curve of recombinant INGAP samples loaded on the same blot (Lanes 1 to 7). The average resulting concentration was 0.103pmol/µl for INGAP-DDK media. A 1nm treatment therefore corresponds to approximately 14.5ul of INGAP-DDK conditioned media diluted in a total volume of 1.5ml of serum-free RPMI medium. The activity of INGAP-DDK, measured via its

capacity to induce Erk 1/2 phosphorylation in rat insulinoma (RIN) cells after a 10 minute treatment period, is expressed as a ratio of phosphorylated Erk 1/2 over total Erk 1/2, normalized to that of untreated controls (Fig. 14). Although there is a clear trend indicating the activation of Erk 1/2 by INGAP-DDK, this result is not statistically different from that of untransfected or empty vector control media treatments. However, these results also indicate that the activity of INGAP DDK is similar to that of recombinant INGAP, especially at the 1nM treatment concentration (Fig.14A).

**Figure 13** Approximate Quantification of INGAP-DDK and INGAP-6His in Conditioned Media from CHO cells Transfected with pCMV6-INGAP (DDK / 6His), by Western Blot.

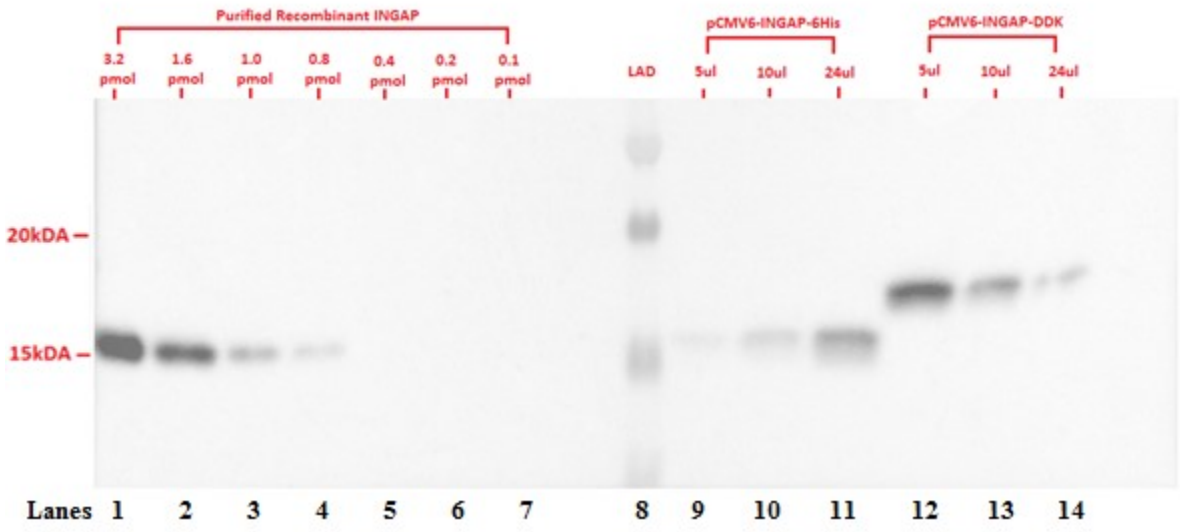

**Figure 14** INGAP-DDK activates Erk 1/2 phosphorylation in RINm5F Cells following a 10-minute treatment at a concentration of 1nm (**A**) and 5nm (**B**).

A

| Treatment | Averaged | SEM |
|---|---|---|
| rINGAP | 1.463802 | 0.484994 |
| INGAP-DDK | 1.415885 | 0.432672 |
| Control Media | 0.973222 | 0.168665 |
| Empty Vector | 0.925639 | 0.193037 |

| Control (No treatment) | 1 |
|---|---|

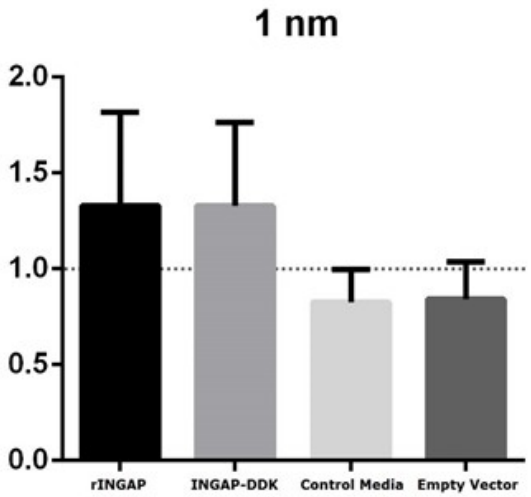


B

| Treatment | Averaged | SEM |
|---|---|---|
| rINGAP | 1.564121 | 0.433334 |
| INGAP-DDK | 1.682934 | 0.462427 |
| Control Media | 1.456298 | 0.363295 |
| Empty Vector | 1.553904 | 0.414175 |

| Control (No treatment) | 1 |
|---|---|

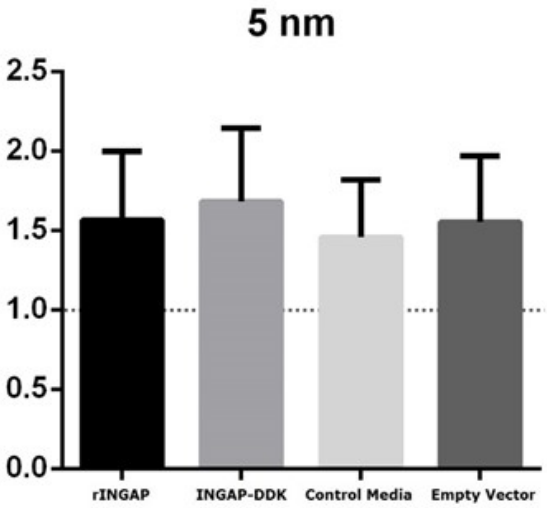

## 3.7 SUB-CLONING OF INGAP-DDK INTO THE AP2 RETROVIRAL PLASMID

Further sub-cloning, using Bgl II and Pme I restriction endonucleases to excise INGAP-DDK DNA from pCMV6-INGAP-DDK, yielded the successful incorporation of the novel INGAP-DDK construct into the AP2 bicistronic retroviral plasmid, also encoding the Green Fluorescent Protein (GFP) downstream of the IRES (Internal Ribosomal Entry Site). The AP2 plasmid was prepared by digestion with Bgl II and BamH I endonucleases, as well as 3' blunting by Mung Bean Nuclease to insure end compatibility, prior to ligation to INGAP-DDK. This newly modified plasmid is referred to as AP2-INGAP-DDK (Fig.15). Initial validation of AP2-INGAP-DDK was performed using a PCR assay with INGAP-specific primers as seen in figure 16, followed by verification of the amplified DNA size by electrophoresis on a 1% agarose gel (Fig.16C). Both of these primers and a sample of AP2-INGAP-DDK were sent to the McGill University Genome Center/Genome Quebec for Sanger sequencing (Fig.17).

**Figure 15** Construct Design Workflow and Restriction Site Overview : AP2-INGAP-DDK

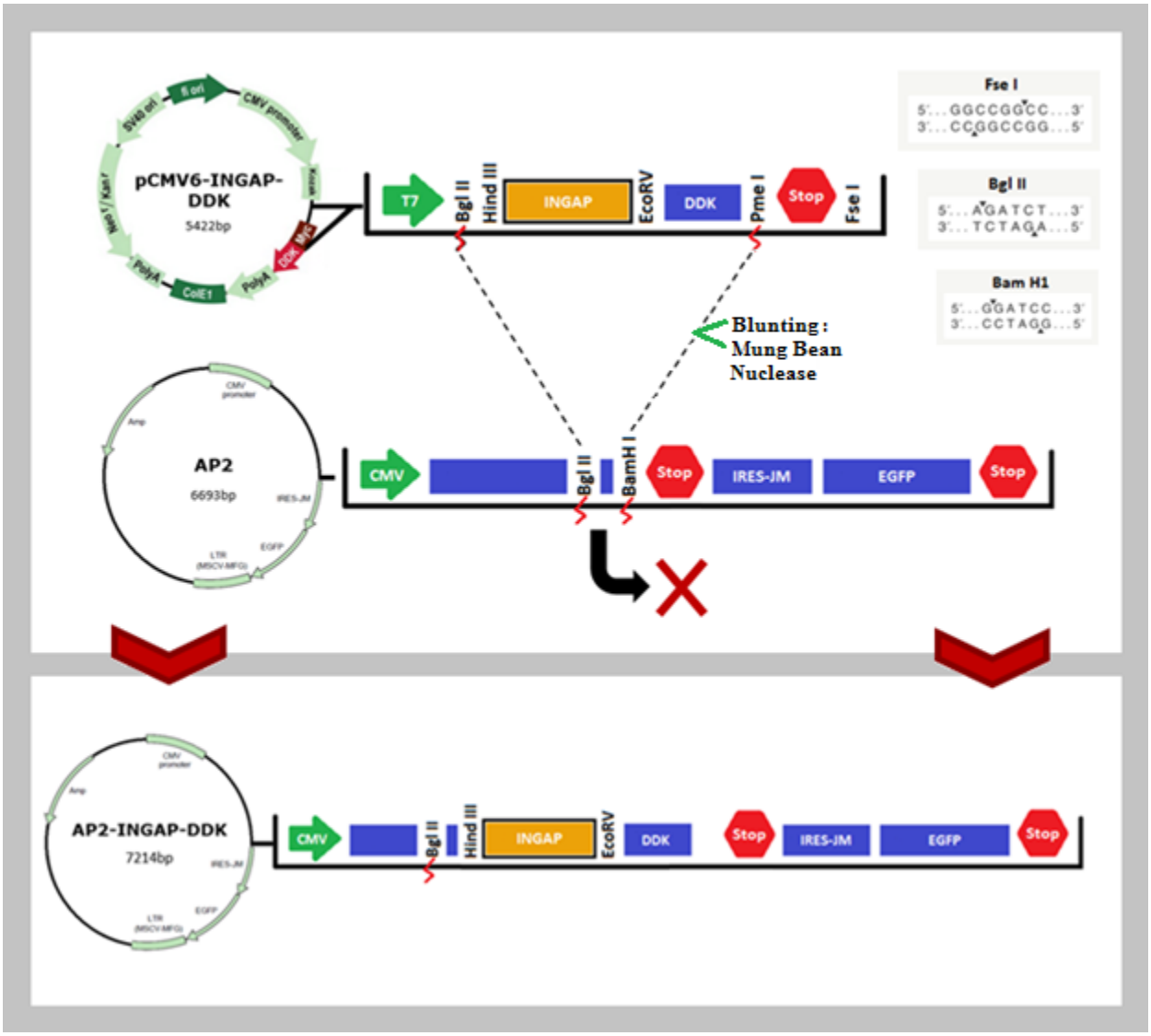

**Figure 16** Verification of INGAP-DDK ligation into AP2 vector by qPCR with INGAP-Specific Primers. Amplification results (**A**) Melt Curve (**B**). Electrophoresis of amplicons on 1% agarose gel (**C**).

**A**

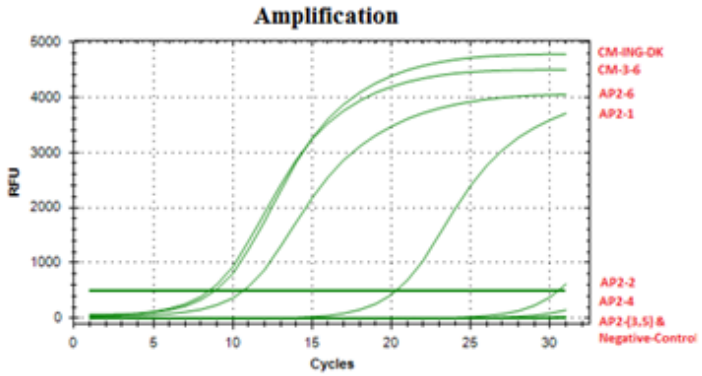


| Well | Fluor | Target | Content | Sample | CQ |
|---|---|---|---|---|---|
| A01 | SYBR | INGAP | Unkn | AP2-1 | 20.30 |
| A02 | SYBR | INGAP | Unkn | AP2-2 | 30.52 |
| A03 | SYBR | INGAP | Unkn | AP2-3 | n/a |
| A04 | SYBR | INGAP | Unkn | AP2-4 | n/a |
| A05 | SYBR | INGAP | Unkn | AP2-5 | n/a |
| A06 | SYBR | INGAP | Unkn | AP2-6 | 10.67 |
| A07 | SYBR | INGAP | Pos Ctrl | CM-3-6 | 8.52 |
| A08 | SYBR | INGAP | Pos Ctrl | CM-ING-DK | 8.89 |
| B01 | SYBR | INGAP | Neg Ctrl | Water | n/a |

**B**

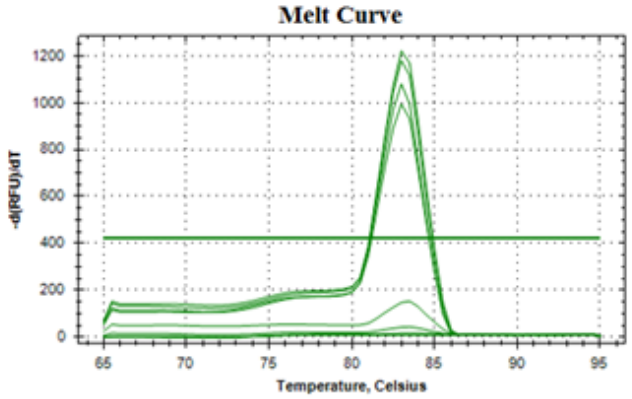


| Well | Fluor | Target | Content | Sample | Melt Temperature | Peak Height |
|---|---|---|---|---|---|---|
| A01 | SYBR | INGAP | Unkn | AP2-1 | 83.00 | 994.10 |
| A02 | SYBR | INGAP | Unkn | AP2-2 | None | None |
| A03 | SYBR | INGAP | Unkn | AP2-3 | None | None |
| A04 | SYBR | INGAP | Unkn | AP2-4 | None | None |
| A05 | SYBR | INGAP | Unkn | AP2-5 | None | None |
| A06 | SYBR | INGAP | Unkn | AP2-6 | 83.00 | 1079.60 |
| A07 | SYBR | INGAP | Pos Ctrl | CM-3-6 | 83.00 | 1178.89 |
| A08 | SYBR | INGAP | Pos Ctrl | CM-ING-DK | 83.00 | 1219.94 |
| B01 | SYBR | INGAP | Neg Ctrl | Water | None | None |

**C**

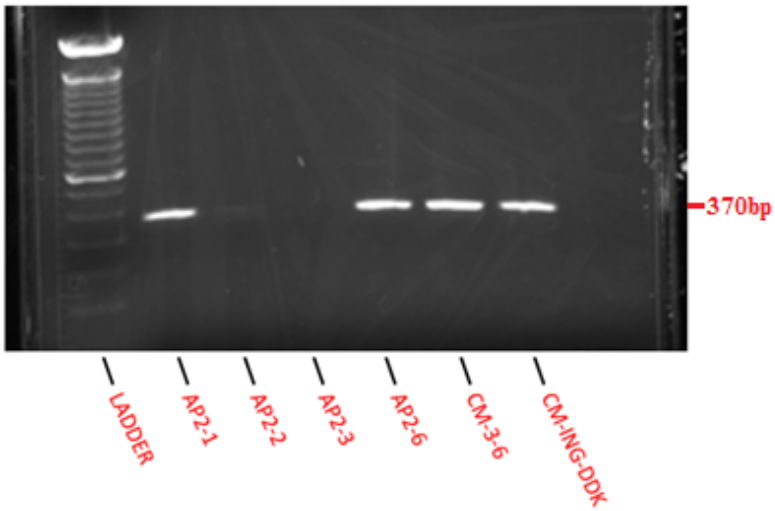

**Figure 17** Results of Sanger Sequencing for the AP2-INGAP-DDK plasmid (AP2-6 sample from figure 17)

**Legend:**

-Correct INGAP
-DDK Tag
-AP2 Vector

ggatcNctcacaacNNNNNggtagatgtcaagaagagNNNNtgggttNNNNNNNgctctgcagaatggcc
aaNNNNtaacgtcggatggccgcgagacggcacctttaaccgagacctcatcacccaggttaagatcaag
gtcttttcacctggcccgcatggacacccagaccaggtcccctacatcgtgacctgggaagccttggctt
ttgacccccctccctgggtcaagccctttgtacaccctaagcctccgcctcctcttcctccatccgcccc
gtctctcccccttgaacctcctcgttcgaccccgcctcgatcctccctttatccagccctcactccttct
ctaggcgccggaattcgttgctaccggactcagatctcaagcttggtaccgagctcggatccagtaccct
tcaccatgatgcttcccatgaccctctgtaggatgtcttggatgctgctttcctgcctgatgttcctttc
ttgggtggaaggtgaagaatctcaaaagaaactgccttcttcacgtataacctgtcctcaaggctctgta
gcctatgggtcctattgctattcactgattttgataccacagacctggtctaatgcagaactatcctgcc
agatgcatttctcaggacacctggcatttcttctcagtactggtgaaattaccttcgtgtcctcccttgt
gaagaacagtttgacggcctaccagtacatctggattggactccatgatccctcacatggtacactaccc
aacggaagtggatggaagtggagcagttccaatgtgctgaccttctataactgggagaggaaccccctcta
ttgctgctgaccgtggttattgtgcagttttgtctcagaaatcaggttttcagaagtggagagattttaa
ttgtgaaaatgagcttccctatatctgcaaattcaaggtcaagggtcaagacaattctgcagatatcctg
gattacaaggatgacgacgataaggtttccccgggctgcaggaattccgcccccccctctcccctcccccc
ccccctaacgtt

**Translated Sequence**

MMLPMTLCRMSWMLLSCLMFLSWVEGEESQKKLPSSRITCPQGSVAYGSYCYSLILI
PQTWSNAELSCQMHFSGHLAFLLSTGEITFVSSLVKNSLTAYQYIWIGLHDPSHGTL
PNGSGWKWSSSNVLTFYNWERNPSIAADRGYCAVLSQKSGFQKWRDFNCENELPYIC
KFKVKGQDNSADILDYKDDDDKVSPGCRNSAPPSPLPPP

# CHAPTER 4: DISCUSSION

## 4.1 EXPRESSION AND SECRETION OF INGAP BY MSCS FOLLOWING GENE TRANSFER.

In the elaboration of this research project, verifying that MSCs can be gene modified to express secrete INGAP is an important step. Although theoretically, cDNA constructs corresponding to any protein can be introduced into any cell line, the capacity for a cell type to transcribe and translate the desired sequence without imparting any unwanted modifications is never a guarantee. Certain cells could possess enzymes that cleave the protein, rendering it useless, or presence of the new protein could drastically alter the cells' physiology, such as making them replicate uncontrollably and therefore unsuitable for treatment purposes. In addition, transcription and translation of a gene product are not a guarantee of secretion, or of the protein localization being as intended, whether in the cytoplasm, nucleus, or membrane bound.

The projected use of MSCs as vehicles for INGAP delivery required full length INGAP to be effectively secreted. In figure 5ABC, Immunohistochemistry of transfected MSCs was able to demonstrate localization of INGAP to the cytoplasm. Furthermore, in CHO and most importantly MSCs cell lines, secretion of INGAP into the conditoned media was demonstrated by Western Blot. See figure 4B, and figure 5 respectively. Interestingly, while INGAP was detected in the Lysates of Cos-1 cells and CHO cells, it could not be detected in those of MSCs. This observation is most likely the result of low transfection efficiency, and short term construct incorporation. While the MSCs do express and secrete INGAP, as demonstrated in figure 5, it is likely that expression is short-lived in the majority of transfected cells, with most of the gene product having been secreted into the surrounding media within the 48 hour transfection period

preceding media collection. However, this does not detract from the overall result : that the cellular machinery of MSCs is capable of producing full length INGAP, as confirmed by the observed molecular weight of the protein (with that of the various tags) corresponding to the expected molecular weight : 17.6kD for INGAP 6-His (Fig.5D). Now that this is known, achieving stable incorporation of the construct is dependant on the technical approach, and not on the overall feasability of the project, which we have demonstrated based on our results.

Obtaining stable INGAP-expressing MSCs through the selection of transfected cells for neomycin resistance, conveyed by the plasmid vector, was attempted using Geneticin G418. This approach has so far been unsuccessful, and very time consuming, prompting the move to a viral transduction approach. A viral vector is expected to lead to a much higher efficiency of gene transfer, up to 80% based on supporting literature, allowing for the production of large quantities of transduced cells through infection with retroviral particles produced by transfected packaging cells [162].

Retroviral vectors, specifically, were chosen on account of our current expertise and use, although lentiviral vectors may also represent a viable alternative, as they possess similar characteristics to retroviruses, but are also capable of transducing non-dividing cells, while retroviruses cannot [163]. However, although a viral approach is beneficial for short term experimentation through to animal studies, its use in human clinical applications may be associated with safety concerns [164]. The pursuit of non-viral constructs should therefore not be abandoned. In primary cell lines, electroporation is generally expected to yield less than 40% efficiency, based on previous studies, while liposomal vectors are often less than 20% effective [165, 166]. However, in this case, liposomal transfection was chosen to conduct the initial

experiments since it was the quickest and most cost-effective way to provide a proof of concept, and since electroporation is often damaging to primary cells [165].

## 4.2 SECRETION OF INGAP BY MESENCHYMAL STEM CELLS

The retroviral plasmid developed in this study could effectively be used to transfer INGAP to nearly any cell type. However, mesenchymal stem cells were chosen as the ideal model for INGAP delivery for a variety of reasons. First, the regenerative potential of MSCs had previously been documented in diabetic disease models, resulting in benefits to insulin/c-peptide production and glucose tolerance [154, 155]. Second, the "homing" properties of MSCs could allow for localized delivery of secreted INGAP following intravenous injection, as the cells migrate with a higher frequency towards sites of inflammation and tissue damage [143, 144]. This effect would further reduce the quantity of INGAP lost in circulation, as delivery may therefore tend to be paracrine. If the INGAP-secreting MSCs were then to differentiate into insulin producing beta-like cells, INGAP could further provide autocrine stimulation or cross-stimulation, further increasing total regeneration. Third, the immunomodulatory properties of MSCs, although inconsequential in chemically-induced *in vivo* models of diabetes, cannot be ignored [167]. The principal hurdle for clinical translation of therapies aimed at treating Type-1 diabetes is the autoimmune nature of the disease itself [34]. Contrary to individuals with Type-2, any newly regenerated beta cells in T1DM patients are susceptible to destruction by the same immune reaction responsible for the disease onset, as they will express the same autoantigens [34, 36]. Therefore, immunomodulation by mesenchymal stem cells may increase survival of new beta cells, without the need for pharmaceutical immunosuppression. Over time, continued

presence of beta cell antigens could lead to the induction of tolerance, in a similar fashion to immunotherapy, where regular antigen doses reduce the severity of allergic reactions [168]. In effect, use of insulin antigen-treated dendritic cells for immunotherapy has been shown to help prevent diabetes onset in NOD mice [169]. The potential of antigen based immunotherapy has also been proposed for human applications [170].

While recent studies have indicated that the main beneficial effect of MSCs is not their differentiation potential, it is important to consider that the application in which we are proposing to use them primarily calls upon their capacity to efficiently secrete INGAP *in situ*, as well as their immunomodulatory and "homing" properties [139, 161, 171]. Any potential for MSCs to acquire insulin expression or differentiate into beta cells *in vivo* is simply an added bonus. In addition, the identity of the cells used herein was not only verified by plastic adherence selection, but also by flow cytometry for MSC specific markers, as published by Dominici et al. [160].

In our study, all experimentation was performed specifically on mouse MSCs, to lay the foundation for future animal studies, necessary before clinical translation of research findings. In laboratory settings, the loss of beta cell mass associated with diabetes is most often modeled using either the chemically induced streptozotocin (STZ) mouse (or rat), or the naturally occuring non-obese diabetic (NOD) mouse [172]. In the STZ model, animals are injected with streptozotocin, a chemical agent toxic to beta cells, and therefore provide an accurate representation of beta cell destruction, decreased insulin/C-peptide, and glucose intolerance, while being free from beta-cell specific autoimmunity [173]. NOD mice, in contrast, do present Type-1 like autoimmunity [174]. MSCs have frequently been used in mouse models, providing a bulk of supporting literature, and the majority of previous INGAP experimentation has been

performed in mice, more specifically the STZ model [118, 147]. For these reasons, mice will provide the ideal choice for *in vivo* testing of INGAP-MSCs, hence the choice of mouse derived MSCs.

There are simple reasons as to why INGAP represents an ideal candidate for cell mediated delivery, and for the treatment of diabetes spectrum diseases in general. To begin, the INGAP protein is relatively small, with a molecular weight of only 16.8kDa, which is conducive to a high efficiency of secretion and favorable pharmacokinetics [175, 176]. By association, INGAP cDNA is short, allowing for a reduced plasmid construct size, thereby improving the efficiency of transfection-based gene-transfer, and insuring efficient packaging within viral particles for transduction based approaches [177]. An even smaller 15aa peptide derivative, representing the active center of INGAP has also been developed, and could be tested in a similar therapeutic approach to the one proposed herein [118]. However, full length INGAP protein was chosen as for this study due to its higher molar efficacy over the peptide, and because the design of short peptide constructs is more challenging, although these will be attempted once a proof of principle with the full length protein is obtained [122]. Cell-mediated delivery of INGAP would prevent localized reactions at the site of subcutaneous injections, as observed in INGAP clinical trials [120]. INGAP is also one of the few known regenerative agents specifically targeting pancreatic beta cells and capable of inducing neogenesis [134]. Supporting research findings in a variety of animal models, and the demonstrated safety and relative efficacy of INGAP in human clinical trials, currently in phase II, make this protein an unmatched candidate for addition to MSC secretome by gene transfer.

In addition to the favorable properties of INGAP, one characteristic makes the use of this protein particularly interesting for human clinical translation. In effect, although INGAP is a constituent of the Reg protein family, even bearing high homology to RegIIIδ, no true homologue of INGAP has yet been identified in humans [178]. However, homologues of INGAP, initially discovered in hamsters, have also been identified in mice [178]. Both of these species have been observed to recover more quickly from insult to the pancreatic islets, compared to their human counterparts, and rodent beta cells proliferate at a much faster rate. The natural presence of INGAP or INGAP-like proteins in these rodents may explain part of the observed difference. Introducing INGAP continuously to the human pancreatic microenvironment, using the methods proposed in this study, may therefore prove all-the-more worthwhile.

At present, it is not known whether INGAP gene-modification of MSCs significantly changes their nature, or simply adds a new secreted gene product, INGAP, to their repertoire. Once stable INGAP-MSCs would be obtained, various experiments would be used to verify if MSCs retain their apparent stemness. To start, unmodified MSCs are capable of differentiating *in vitro* into osteocytes, by growth in the presence of 100nM dexamethasone, 200μM L-ascorbic acid-2-phosphate and 10mM β-glycerol phosphate for 21days, and into adipocytes, by growth in the presence of 50μmol/L indomethacin, 10μM insulin, 1μmol/L dexamethasone, and 0.5mM 3-isobutyl-L-methyl-xanthine for 14 days [179]. INGAP MSCs would be subjected to the same condition, as an assessment of their differentiation potential, as we have verified with other gene-modified MSCs [147].

Considering that the retroviral plasmid proposed as a vector herein encompasses GFP fluorescence, it could be modified to include other markers such as luciferase. GFP-positive INGAP MSCs could be detected during histological analysis following any *in vivo* studies. The cell's morphology, localization, and expression (detectable by fluorescent in-situ hybridization) at various time points following *in vivo* administration would provide clues as to the general direction of differentiation, or overall cell fate. MSCs may have the capability to differentiate into insulin producing cells while retaining INGAP expression, thereby integrating into the islets and locally stimulating beta cell mass expansion through paracrine and autocrine signaling.

## 4.3 CHOICE OF TAGS, PLASMIDS AND RESTRICTION SITES.

The DDK (FLAG) tag was chosen over the previous 6-His and V5 C-terminal tags for a variety of reasons. First, the V5 tag was removed due to its high molecular weight, which would have made the overall construct significantly more bulky, potentially impairing integration into virions during retroviral transduction. The size of cDNA which can be incorporated into retroviral virions is limited, in comparison to other virus types [180]. In contrast to V5, DDK (FLAG) has a very low molecular weight of only 1.01kD [181]. Second, initial experiments using anti-6His antibodies upon lysates from the transfection of Cos-1 cells with INGAP-6His cDNA produced a "dirty" Western Blot, exposing non-specific binding which reduced visibility of the actual tagged INGAP signal. Specificity of detection is paramount for the collection of accurate results, especially if tagged INGAP is to be eventually detected by immunohistochemistry in the tissue of animal models treated with INGAP-MSCs, where staining would not only be used to confirm presence of the protein, but also its localization and

distribution throughout tissue. In contrast, the DDK (FLAG) tag has been demonstrated to have very high specificity, and is absent from naturally occurring proteins, making it ideal for these applications [181]. Third, this tag is frequently used in applications involving mammalian cells and proteins, meaning a range of specific antibodies used for its recognition are readily available [182]. Additionally, DDK is highly soluble, a crucial benefit in the context of tagging a secreted protein, which needs to, in-turn, be highly soluble for efficient transport in plasma [181, 183]. A study completed by Schmidt et al. has suggested that a post-translational modification occurring in certain cell lines, which consists of Tyrosine sulfation, can inhibit the recognition of DDK tags in secreted proteins [182]. As demonstrated in figure 11B, DDK tagging of INGAP expressed by CHOs produces a strong signal on Western Blots probed with specific anti-DDK antibody (Origene, MD, USA), indicating that this undesirable post-translational modification does not likely occur in these situations. DDK tagging is therefore a viable and efficient means of INGAP tagging during gene-modification of MSCs.

In the assay of INGAP-DDK, the results of which are shown in figure 14, INGAP-DDK appeared to upregulate Erk 1/2 phosphorylation in comparison to empty vector, simple conditioned media, and untreated negative controls. While this difference seems to be most noticeable in the 1nm treatment groups, a statistically significant result could not be established for either treatment concentration. An important consideration for this experiment is that the concentrations of these treatments, while relatively exact for rINGAP, are only approximate for INGAP-DDK, since conditioned media was only roughly quantified by the comparison of band volumes to those of a standard curve by Western Blot. Further data points will be required to achieve statistical significance and to reduce the effects of confounding factors such as errors in cell manipulation, as this experiment is highly dependent upon the RIN cells being subjected to

each experimental step for identical amounts of time. Growth factors present in Opti-MEM medium, used throughout the RIN cell treatment step, may also skew results. In the future, when INGAP-DDK is purified and more precisely quantified, these trends could be established with greater accuracy.

Both starting plasmids, pcDNA 3.1D-V5-6His, with the 1-1 INGAP construct and the 3-6 INGAP construct, were utilized for initial experimentation because they both had already been validated to induce INGAP expression by the transfection of immortal cell lines. The size difference between both constructs further provided visual evidence of INGAP's presence upon analysis of Western Blot results, ruling out the possibility of false-positives, as seen in figure 3 and figure 4.

When deciding to modify the INGAP construct with a DDK (FLAG) tag, the choice of vector was given careful consideration. pCMV6 was chosen primarily because of its possession of the DDK tag, but more specifically because this tag was located immediately downstream of two restriction sites, EcoRV and Hind III, which were compatible to those present on the 5' and 3' ends of INGAP within pcDNA 3.1D-V5-6His, as demonstrated in figure 9. Additional benefits of pCMV6 are its small size, 621bp shorter than pcDNA 3.1D-V5-6His when both plasmids contain INGAP, which is conducive to higher transfection efficiency. Antibiotic selection was used to isolate positive DH5α colonies after transformation throughout the sub-cloning process. Since pCMV6 encodes a Kanamycin resistance gene, and pcDNA 3.1D incorporates an Ampicillin resistance gene, the difference in antibiotic selection was used to prevent contamination from the source pcDNA 3.1D-V5-6His vector during subcloning. This safeguard was also utilized in the sub-cloning of INGAP-DDK to AP2, where colonies were

screened for Ampicillin resistance, inherent to AP2, preventing pCMV6 colonies, which only bear Kanamycin resistance, from growing.

In choosing a plasmid for viral transduction approaches, AP2 proved ideal. This retroviral vector contains green fluorescent protein (GFP), for use in cell tracking applications. Additionally, use of this plasmid for transduction of mesenchymal stem cells had already been validated by our collaborators, Eliopoulos et al., using the erythropoietin EPO gene [184]. Furthermore, as evidenced by figure 15 the Bgl II and BamH I restriction sites present upstream of IRES, and downstream of the CMV promoter allow for incorporation of the INGAP-DDK construct without disrupting any of the other required sequences. The Bgl II site is also present upstream of INGAP-DDK in pCMV6, but a concession, in the form of a blunting step using Mung-Bean nuclease, was required to accomodate the incompatible downstream restriction site in the preparation of the vector DNA. Blunting of the AP2 vector's 3' end, during the sub-cloning process, resulted in the removal of the BamH I restriction site, preventing the use of restriction digestion to confirm incorporation of the construct. For this reason, the sub-cloning of INGAP-DDK into the multiple cloning site (MCS) of AP2, upstream of GFP, was validated by PCR amplification using INGAP-specific primers, shown in figures 16, and later by Sanger Sequencing (Fig.17).

## 4.4 PERSPECTIVES ON GENE/CELL THERAPY

There are many issues to consider before regenerative cell therapy can be widely applied to the treatment of diabetes. The most important consideration is the fine equiblibrium between treatment efficacy and treatment safety. In undertaking a regenerative approach, one must

acknowledge that the injection of cells/stem cells that have undergone prolonged expansion in culture may pose a health risk, and could have the potential to induce tumorigenesis [185]. However, numerous precautions and safeguards can be implemented, such as karyotyping the cells prior to injection, careful examination of secretome and gene expression profiles, and conducting differentiation and growth rate assays to help exclude any problematic cultures [186, 187].

Carefully planned animal studies, designed to closely mimick the expected human physiological interactions, are also crucial to discovering and understanding any unexpected physiological effects of a new treatment. Nevertheless, the important species barrier abolishes the guarantee of successful clinical translation. When considering diabetes specifically, although the treatment objectives for Type-1 and Type-2 are similar : restoring beta cell mass and normal glycemic patterns, significant pathophysiological difference exist between both types [30, 38]. Even when a treatment approach can be used to treat both, dosages, routes of administration, frequency, side-effects, and benefits may all drastically differ [188]. In type-1 the most imposing hurdle lies with the autoimmune response against the islets [30]. Even if efficient regeneration can be achieved, recovery may not persist unless either the autoimmune response is reduced, or treatment is continuous [34, 120]. The latter option is less desirable due to its impact on patient lifestyle, unless it can be completed automatically, without patient involvement, such as in the case of cell-mediated drug delivery. It is for this reason that we have oriented our efforts towards a combinatorial INGAP-MSC therapy, with the objective of modulating the immune response using the properties of MSCs, and allowing both INGAP and MSCs to stimulate regeneration in a continuous fashion.

In Type-2 diabetes, although the recovery of beta-cell mass may be significantly less challenging, due to absence of autoimmunity, this does not guarantee complete recovery in patients [120]. Beta cell regeneration does not eliminate peripheral insulin resistance, often directly caused by patient lifestyle factors [38]. Elevation of blood glucose levels could still cause complications in these circumstances, although the increase in circulating C-peptide from endogenous insulin production would likely still provide benefits, due to its association with vascular endothelial health [51, 189]. Type-2 diabetics recieving regenerative therapy would therefore benefit from an intensive treatment plan including dietary and exercise considerations. When recapitulating all the treatment aspects of diabetes, it increasingly clear that a cure based on regenative therapies must also take into account other complex physiological interactions outside of the islet environment, such as tolerance failure and peripheral insulin resistance.

## 4.5 CONCLUSIONS

From the initial hypothesis and aims of this thesis, to the experiments subsequently performed and the interpretation of the results, the following conclusions can be made:

1. Mouse bone marrow-derived Mesenchymal stem cells can effectively be transfected so as to express and secrete INGAP.

2. DDK (FLAG)-tagging of INGAP cDNA provides a reliable and compact means of detection.

3. A retroviral plasmid containing INGAP cDNA has been produced for future transduction of MSCs, or any other desirable cell line, with tagged INGAP cDNA and cellular expression of Green-Fluorescent Protein, useful for both cell tracking and cell sorting applications.

## 4.6 FUTURE DIRECTIONS

While this study has demonstrated the feasibility of INGAP delivery through MSCs, and developed the tools necessary to generate stable INGAP-expressing cell lines, many avenues remain to be explored, before INGAP-MSCs can be considered clinically relevant. Followup experiments should focus first, upon the production of retrovirally transduced INGAP-MSCs, and next, upon the characterization of the enhanced MSC secretome, via enzyme-linked immuno-assay (ELISA), and co-culture of INGAP-MSCs with rat insulinoma or human pancreatic ductal epithelial (HPDE) cell lines, as *in vitro* model of beta cells, using a transwell. Transduced cell lines should undergo selection to isolate high expressing cells and increase

overall INGAP production, which may allow for the use of fewer cells during eventual treatment. These cells should additionally be karyotyped to insure the prevention of tumorgenesis during *in vivo* experiments. These *in vivo* experiments can be performed using the same model used for the development of INGAP: the Streptozotocin (STZ) induced diabetic mouse model, which provides a significant representation of islet response to treatment while being free from confounding immunological factors. Although viral transduction is a rapid and effective means of achieving incorporation of the INGAP cDNA, further optimization of lipofection protocols, or other non-viral approaches should not be neglected, as many have already been approved for human clinical use.

## 4.7 SIGNIFICANCE

This is the first study to propose combinatorial therapy using both INGAP and Stem Cells (of any kind), and also the first to propose cell-based delivery of INGAP as a means of remedying the apparent short half-life of this protein in serum. When taking into account the promising results achieved by simple INGAP injections, going as far as human clinical trials, demonstrating the feasibility of INGAP expressing MSCs is a first step in the development of a high efficiency INGAP-based treatment, which could eventually lead to curative therapies for diabetes of types 1 and 2.

# REFERENCES


1. Kimura, W., *Surgical anatomy of the pancreas for limited resection.* J Hepatobiliary Pancreat Surg, 2000. **7**(5): p. 473-9.

2. Slack, J.M., *Developmental biology of the pancreas.* Development, 1995. **121**(6): p. 1569-80.

3. Mourad, N., et al., *The venous drainage of the pancreas.* Surg Radiol Anat, 1994. **16**(1): p. 37-45.

4. Okahara, M., et al., *Arterial supply to the pancreas; variations and cross-sectional anatomy.* Abdom Imaging, 2010. **35**(2): p. 134-42.

5. Ibukuro, K., *Vascular anatomy of the pancreas and clinical applications.* Int J Gastrointest Cancer, 2001. **30**(1-2): p. 87-104.

6. Chandra, R. and R.A. Liddle, *Neural and Hormonal Regulation of Pancreatic Secretion.* Current opinion in gastroenterology, 2009. **25**(5): p. 441-446.

7. Jarhult, J., et al., *The functional importance of sympathetic nerves to the liver and endocrine pancreas.* Ann Surg, 1979. **189**(1): p. 96-100.

8. Mastracci, T.L. and L. Sussel, *The Endocrine Pancreas: insights into development, differentiation and diabetes.* Wiley interdisciplinary reviews. Membrane transport and signaling, 2012. **1**(5): p. 609-628.

9. Pallagi, P., P. Hegyi, and Z. Rakonczay, Jr., *The Physiology and Pathophysiology of Pancreatic Ductal Secretion: The Background for Clinicians.* Pancreas, 2015. **44**(8): p. 1211-33.

10. Hagai, H., *Configurational anatomy of the pancreas: its surgical relevance from ontogenetic and comparative-anatomical viewpoints.* J Hepatobiliary Pancreat Surg, 2003. **10**(1): p. 48-56.

11. Dawson, P.M. and T.G. Allen-Mersh, *The anatomical relationship between the retropancreatic part of the bile duct and the main pancreatic duct.* Annals of The Royal College of Surgeons of England, 1983. **65**(3): p. 188-190.

12. Keller, J. and P. Layer, *Human pancreatic exocrine response to nutrients in health and disease.* Gut, 2005. **54**(Suppl 6): p. 1-28.

13. Weir, G.C. and S. Bonner-Weir, *Islet β cell mass in diabetes and how it relates to function, birth, and death.* Annals of the New York Academy of Sciences, 2013. **1281**(1): p. 92-105.

14. Engelking, L.R., *Physiology of the endocrine pancreas.* Semin Vet Med Surg (Small Anim), 1997. **12**(4): p. 224-9.

15. Ballian, N. and F.C. Brunicardi, *Islet vasculature as a regulator of endocrine pancreas function.* World J Surg, 2007. **31**(4): p. 705-14.

16. Chandra, R. and R.A. Liddle, *Recent advances in pancreatic endocrine and exocrine secretion.* Current opinion in gastroenterology, 2011. **27**(5): p. 439-443.

17. Kim, A., et al., *Islet architecture: A comparative study.* Islets, 2009. **1**(2): p. 129-36.

18. Bosco, D., et al., *Unique arrangement of alpha- and beta-cells in human islets of Langerhans.* Diabetes, 2010. **59**(5): p. 1202-10.

19. Holmes, R., *Carbohydrate digestion and absorption.* Journal of Clinical Pathology. Supplement (Royal College of Pathologists). 1971. **5**: p. 10-13.

20. Southgate, D.A., *Digestion and metabolism of sugars.* Am J Clin Nutr, 1995. **62**(1 Suppl): p. 203S-210S; discussion 211S.

21. Thorens, B. and M. Mueckler, *Glucose transporters in the 21st Century.* American Journal of Physiology - Endocrinology and Metabolism, 2010. **298**(2): p. E141-E145.

22. Vannucci, S.J., F. Maher, and I.A. Simpson, *Glucose transporter proteins in brain: delivery of glucose to neurons and glia.* Glia, 1997. **21**(1): p. 2-21.

23. Barnard, R.J. and J.F. Youngren, *Regulation of glucose transport in skeletal muscle.* Faseb j, 1992. **6**(14): p. 3238-44.

24. Zierler, K., *Whole body glucose metabolism.* Am J Physiol, 1999. **276**(3 Pt 1): p. E409-26.

25. Kulkarni, R.N., *The islet β-cell.* The International Journal of Biochemistry & Cell Biology, 2004. **36**(3): p. 365-371.

26. MacDonald, P.E., J.W. Joseph, and P. Rorsman, *Glucose-sensing mechanisms in pancreatic β-cells.* Philosophical Transactions of the Royal Society B: Biological Sciences, 2005. **360**(1464): p. 2211-2225.

27. Kanno, T., P. Rorsman, and S.O. Gopel, *Glucose-dependent regulation of rhythmic action potential firing in pancreatic beta-cells by K(ATP)-channel modulation.* J Physiol, 2002. **545**(Pt 2): p. 501-7.

28. Fridlyand, L.E., D.A. Jacobson, and L.H. Philipson, *Ion channels and regulation of insulin secretion in human β-cells: A computational systems analysis.* Islets, 2013. **5**(1): p. 1-15.

29. Atkinson, M.A., *The Pathogenesis and Natural History of Type 1 Diabetes.* Cold Spring Harbor Perspectives in Medicine, 2012. **2**(11): p. a007641.

30. Gillespie, K.M., *Type 1 diabetes: pathogenesis and prevention.* Cmaj, 2006. **175**(2): p. 165-70.

31. Romagnani, S., *Immunological tolerance and autoimmunity.* Intern Emerg Med, 2006. **1**(3): p. 187-96.

32. Xing, Y. and K.A. Hogquist, *T-Cell Tolerance: Central and Peripheral.* Cold Spring Harbor Perspectives in Biology, 2012. **4**(6): p. a006957.

33. Ring, G.H. and F.G. Lakkis, *Breakdown of self-tolerance and the pathogenesis of autoimmunity.* Semin Nephrol, 1999. **19**(1): p. 25-33.

34. Kuhn, C., et al., *Regulatory mechanisms of immune tolerance in type 1 diabetes and their failures.* J Autoimmun, 2016. **71**: p. 69-77.

35. Yagi, H., et al., *Analysis of the roles of CD4+ and CD8+ T cells in autoimmune diabetes of NOD mice using transfer to NOD athymic nude mice.* Eur J Immunol, 1992. **22**(9): p. 2387-93.

36. Roep, B.O. and M. Peakman, *Antigen Targets of Type 1 Diabetes Autoimmunity.* Cold Spring Harbor Perspectives in Medicine, 2012. **2**(4): p. a007781.

37. Klonoff, D.C., *The Increasing Incidence of Diabetes in the 21st Century.* Journal of diabetes science and technology (Online), 2009. **3**(1): p. 1-2.

38. Scheen, A.J., *Pathophysiology of type 2 diabetes.* Acta Clin Belg, 2003. **58**(6): p. 335-41.

39. Pawlak, J. and R.A. Derlacz, *[The mechanism of insulin resistance in peripheral tissues].* Postepy Biochem, 2011. **57**(2): p. 200-6.

40. Cerf, M.E., *Beta Cell Dysfunction and Insulin Resistance.* Frontiers in Endocrinology, 2013. **4**: p. 37.

41. Chan, C.B., et al., *Glucose-inducible hypertrophy and suppression of anion efflux in rat beta cells.* J Endocrinol, 2002. **173**(1): p. 45-52.

42. Kushner, J.A., *The role of aging upon beta cell turnover.* J Clin Invest, 2013. **123**(3): p. 990-5.

43. Lim, E.L., et al., *Reversal of type 2 diabetes: normalisation of beta cell function in association with decreased pancreas and liver triacylglycerol.* Diabetologia, 2011. **54**(10): p. 2506-2514.

44. Ades, P.A., et al., *Remission of recently diagnosed type 2 diabetes mellitus with weight loss and exercise.* J Cardiopulm Rehabil Prev, 2015. **35**(3): p. 193-7.

45. Forbes, J.M. and M.E. Cooper, *Mechanisms of diabetic complications.* Physiol Rev, 2013. **93**(1): p. 137-88.

46. Schade, D.S. and R.P. Eaton, *Diabetic ketoacidosis--pathogenesis, prevention and therapy.* Clin Endocrinol Metab, 1983. **12**(2): p. 321-38.

47. Kalra, S., et al., *Hypoglycemia: The neglected complication.* Indian Journal of Endocrinology and Metabolism, 2013. **17**(5): p. 819-834.

48. Chawla, A., R. Chawla, and S. Jaggi, *Microvasular and macrovascular complications in diabetes mellitus: Distinct or continuum?* Indian Journal of Endocrinology and Metabolism, 2016. **20**(4): p. 546-551.

49. Pendsey, S.P., *Understanding diabetic foot.* International Journal of Diabetes in Developing Countries, 2010. **30**(2): p. 75-79.

50. Ghorbani, A. and R. Shafiee-Nick, *Pathological consequences of C-peptide deficiency in insulin-dependent diabetes mellitus.* World Journal of Diabetes, 2015. **6**(1): p. 145-150.

51. Ido, Y., et al., *Prevention of vascular and neural dysfunction in diabetic rats by C-peptide.* Science, 1997. **277**(5325): p. 563-6.

52. Sari, R. and M.K. Balci, *Relationship between C peptide and chronic complications in type-2 diabetes mellitus.* Journal of the National Medical Association, 2005. **97**(8): p. 1113-1118.

53. Greiver, M., et al., *Prevalence and epidemiology of diabetes in Canadian primary care practices: a report from the Canadian Primary Care Sentinel Surveillance Network.* Can J Diabetes, 2014. **38**(3): p. 179-85.

54. Seuring, T., O. Archangelidi, and M. Suhrcke, *The Economic Costs of Type 2 Diabetes: A Global Systematic Review.* Pharmacoeconomics, 2015. **33**(8): p. 811-31.

55. *Worldwide trends in diabetes since 1980: a pooled analysis of 751 population-based studies with 4.4 million participants.* Lancet, 2016. **387**(10027): p. 1513-30.

56. Rosenfeld, L., *Insulin: discovery and controversy.* Clin Chem, 2002. **48**(12): p. 2270-88.

57. Giordano, C., *Insulin therapy: unmet needs and new perspectives.* Minerva Endocrinol, 2013. **38**(1): p. 95-102.

58. Banting, F.G., B.C. Herbert, and C.J. Bertram, *Extract obtainable from the mammalian pancreas or from the related glands in fishes, useful in the treatment of diabetes mellitus, and a method of preparing it*. 1923, Google Patents.

59. Quianzon, C.C. and I. Cheikh, *History of insulin.* Journal of Community Hospital Internal Medicine Perspectives, 2012. **2**(2): p. 10.3402/jchimp.v2i2.18701.

60. Poulsen, C., L. Langkjaer, and C. Worsoe, *Precipitation of insulin products used for continuous subcutaneous insulin infusion.* Diabetes Technol Ther, 2005. **7**(1): p. 142-50.

61. L, J.R., *Process for purifying insulin*. 1975, Google Patents.

62. The, M.J., *Human insulin: DNA technology's first drug.* Am J Hosp Pharm, 1989. **46**(11 Suppl 2): p. S9-11.

63. Goeddel, D.V., D.G. Kleid, and K. Itakura, *Human proinsulin and analogs thereof and method of preparation by microbial polypeptide expression and conversion thereof to human insulin*. 1982, Google Patents.

64. Reece, S.W. and C.L. Hamby Williams, *Insulin Pump Class: Back to the Basics of Pump Therapy.* Diabetes Spectrum : A Publication of the American Diabetes Association, 2014. **27**(2): p. 135-140.

65. Rupp, W.M., et al., *The use of an implantable insulin pump in the treatment of type II diabetes.* N Engl J Med, 1982. **307**(5): p. 265-70.

66. Andrews, S., et al., *Transdermal Insulin Delivery Using Microdermabrasion.* Pharmaceutical research, 2011. **28**(9): p. 2110-2118.

67. Meyer, B.R., et al., *Transdermal delivery of human insulin to albino rabbits using electrical current.* Am J Med Sci, 1989. **297**(5): p. 321-5.

68. Hisasue, J., et al., *Inhalative administration of insulin using a new bubble jet atomization device.* Fukuoka Igaku Zasshi, 2011. **102**(6): p. 215-22.

69. Fonte, P., et al., *Oral insulin delivery: how far are we?* J Diabetes Sci Technol, 2013. **7**(2): p. 520-31.

70. Cefalu, W.T. and S. Urquhart, *Clinical management strategies for type 2 diabetes.* Jaapa, 2007. **Suppl**: p. 9-14.

71. Harrigan, R.A., M.S. Nathan, and P. Beattie, *Oral agents for the treatment of type 2 diabetes mellitus: pharmacology, toxicity, and treatment.* Ann Emerg Med, 2001. **38**(1): p. 68-78.

72. Sirtori, C.R. and C. Pasik, *Re-evaluation of a biguanide, metformin: mechanism of action and tolerability.* Pharmacol Res, 1994. **30**(3): p. 187-228.

73. Hauner, H., *The mode of action of thiazolidinediones.* Diabetes Metab Res Rev, 2002. **18 Suppl 2**: p. S10-5.

74. Melander, A., *Clinical pharmacology of sulfonylureas.* Metabolism, 1987. **36**(2 Suppl 1): p. 12-6.

75. Koster, J.C., Q. Sha, and C.G. Nichols, *Sulfonylurea and K(+)-Channel Opener Sensitivity of K(ATP) Channels: Functional Coupling of Kir6.2 and Sur1 Subunits.* The Journal of General Physiology, 1999. **114**(2): p. 203-213.

76. Sunaga, Y., et al., *The effects of mitiglinide (KAD-1229), a new anti-diabetic drug, on ATP-sensitive K+ channels and insulin secretion: comparison with the sulfonylureas and nateglinide.* Eur J Pharmacol, 2001. **431**(1): p. 119-25.

77. Derosa, G. and P. Maffioli, *α-Glucosidase inhibitors and their use in clinical practice.* Archives of Medical Science : AMS, 2012. **8**(5): p. 899-906.

78. Hansen, K.B., T. Vilsbøll, and F.K. Knop, *Incretin mimetics: a novel therapeutic option for patients with type 2 diabetes – a review.* Diabetes, metabolic syndrome and obesity : targets and therapy, 2010. **3**: p. 155-163.

79. Prasad-Reddy, L. and D. Isaacs, *A clinical review of GLP-1 receptor agonists: efficacy and safety in diabetes and beyond.* Drugs in Context, 2015. **4**: p. 212283.

80. Gruessner, R.W.G. and A.C. Gruessner, *Pancreas Transplant Alone: A procedure coming of age.* Diabetes Care, 2013. **36**(8): p. 2440-2447.

81. Luzi, L., *Pancreas transplantation and diabetic complications.* N Engl J Med, 1998. **339**(2): p. 115-7.

82. Redfield, R.R., J.R. Scalea, and J.S. Odorico, *Simultaneous pancreas and kidney transplantation: current trends and future directions.* Current Opinion in Organ Transplantation, 2015. **20**(1): p. 94-102.

83. Kimelman, M. and G. Brandacher, *Trends in immunosuppression after pancreas transplantation: what is in the pipeline?* Curr Opin Organ Transplant, 2013. **18**(1): p. 76-82.

84. Marroquin, C.E., et al., *Half-life analysis of pancreas and kidney transplants.* Transplantation, 2005. **80**(2): p. 272-5.

85. Montiel-Casado, M.C., et al., *Pancreas graft survival in simultaneous pancreas-kidney versus pancreas-after-kidney and pancreas alone transplantations: a single institution experience.* Transplant Proc, 2013. **45**(10): p. 3609-11.

86. Shapiro, A.M.J., et al., *Islet Transplantation in Seven Patients with Type 1 Diabetes Mellitus Using a Glucocorticoid-Free Immunosuppressive Regimen.* New England Journal of Medicine, 2000. **343**(4): p. 230-238.

87. Srinivasan, P., et al., *Islet cell transplantation.* Postgraduate Medical Journal, 2007. **83**(978): p. 224-229.

88. Barton, F.B., et al., *Improvement in Outcomes of Clinical Islet Transplantation: 1999–2010.* Diabetes Care, 2012. **35**(7): p. 1436-1445.

89. Maffi, P. and A. Secchi, *Clinical results of islet transplantation.* Pharmacol Res, 2015. **98**: p. 86-91.

90. Bonner-Weir, S., et al., *β-Cell Growth and Regeneration: Replication Is Only Part of the Story.* Diabetes, 2010. **59**(10): p. 2340-2348.

91. Cigliola, V., et al., *Stress-induced adaptive islet cell identity changes.* Diabetes Obes Metab, 2016. **18 Suppl 1**: p. 87-96.

92. Paris, M., et al., *Review: pancreatic beta-cell neogenesis revisited.* Exp Diabesity Res, 2004. **5**(2): p. 111-21.

93. Lu, J., et al., *Transdifferentiation of pancreatic α-cells into insulin-secreting cells: From experimental models to underlying mechanisms.* World Journal of Diabetes, 2014. **5**(6): p. 847-853.

94. Minami, K. and S. Seino, *Pancreatic acinar-to-beta cell transdifferentiation in vitro.* Front Biosci, 2008. **13**: p. 5824-37.

95. Thorel, F., et al., *Conversion of adult pancreatic alpha-cells to beta-cells after extreme beta-cell loss.* Nature, 2010. **464**(7292): p. 1149-54.

96. Chera, S., et al., *Diabetes recovery by age-dependent conversion of pancreatic delta-cells into insulin producers.* Nature, 2014. **514**(7523): p. 503-7.

97. Song, K.H., et al., *In vitro transdifferentiation of adult pancreatic acinar cells into insulin-expressing cells.* Biochem Biophys Res Commun, 2004. **316**(4): p. 1094-100.

98. Okuno, M., et al., *Generation of insulin-secreting cells from pancreatic acinar cells of animal models of type 1 diabetes.* American Journal of Physiology - Endocrinology And Metabolism, 2007. **292**(1): p. E158.

99. Minami, K., et al., *Lineage tracing and characterization of insulin-secreting cells generated from adult pancreatic acinar cells.* Proceedings of the National Academy of Sciences of the United States of America, 2005. **102**(42): p. 15116-15121.

100. Reichert, M. and A.K. Rustgi, *Pancreatic ductal cells in development, regeneration, and neoplasia.* The Journal of Clinical Investigation, 2011. **121**(12): p. 4572-4578.

101. Bonner-Weir, S., et al., *In vitro cultivation of human islets from expanded ductal tissue.* Proc Natl Acad Sci U S A, 2000. **97**(14): p. 7999-8004.

102. Dirice, E., et al., *Inhibition of DYRK1A Stimulates Human beta-Cell Proliferation.* Diabetes, 2016. **65**(6): p. 1660-71.

103. Boerner, B.P., et al., *WS6 induces both alpha and beta cell proliferation without affecting differentiation or viability.* Endocr J, 2015. **62**(4): p. 379-86.

104. Shen, W., et al., *Small-molecule inducer of beta cell proliferation identified by high-throughput screening.* J Am Chem Soc, 2013. **135**(5): p. 1669-72.

105. Annes, J.P., et al., *Adenosine kinase inhibition selectively promotes rodent and porcine islet β-cell replication.* Proceedings of the National Academy of Sciences of the United States of America, 2012. **109**(10): p. 3915-3920.

106. Chen, S., et al., *A small molecule that directs differentiation of human ESCs into the pancreatic lineage.* Nat Chem Biol, 2009. **5**(4): p. 258-65.

107. Thatava, T., et al., *Indolactam V/GLP-1-mediated Differentiation of Human iPS Cells into Glucose-Responsive Insulin-Secreting Progeny.* Gene therapy, 2011. **18**(3): p. 283-293.

108. Song, I., et al., *Beta Cell Mass Restoration in Alloxan-Diabetic Mice Treated with EGF and Gastrin.* PLoS One, 2015. **10**(10): p. e0140148.

109. Song, Z., et al., *Epidermal Growth Factor Receptor Signaling Regulates beta Cell Proliferation in Adult Mice.* J Biol Chem, 2016. **291**(43): p. 22630-22637.

110. Oh, Y.S., et al., *Betacellulin-induced beta cell proliferation and regeneration is mediated by activation of ErbB-1 and ErbB-2 receptors.* PLoS One, 2011. **6**(8): p. e23894.

111. Rooman, I., J. Lardon, and L. Bouwens, *Gastrin stimulates beta-cell neogenesis and increases islet mass from transdifferentiated but not from normal exocrine pancreas tissue.* Diabetes, 2002. **51**(3): p. 686-90.

112. Buteau, J., *GLP-1 receptor signaling: effects on pancreatic beta-cell proliferation and survival.* Diabetes Metab, 2008. **34 Suppl 2**: p. S73-7.

113. Liu, M.J., et al., *Prolonged remission of diabetes by regeneration of beta cells in diabetic mice treated with recombinant adenoviral vector expressing glucagon-like peptide-1.* Mol Ther, 2007. **15**(1): p. 86-93.

114. Habener, J.F. and V. Stanojevic, *alpha-cell role in beta-cell generation and regeneration.* Islets, 2012. **4**(3): p. 188-98.

115. Rosenberg, L., W.P. Duguid, and A.I. Vinik, *The effect of cellophane wrapping of the pancreas in the Syrian golden hamster: autoradiographic observations.* Pancreas, 1989. **4**(1): p. 31-7.

116. Rosenberg, L., R.A. Brown, and W.P. Duguid, *A new approach to the induction of duct epithelial hyperplasia and nesidioblastosis by cellophane wrapping of the hamster pancreas.* The Journal of surgical research, 1983. **35**(1): p. 63-72.

117. Rafaeloff, R., et al., *Cloning and sequencing of the pancreatic islet neogenesis associated protein (INGAP) gene and its expression in islet neogenesis in hamsters.* J Clin Invest, 1997. **99**(9): p. 2100-9.

118. Rosenberg, L., et al., *A pentadecapeptide fragment of islet neogenesis-associated protein increases beta-cell mass and reverses diabetes in C57BL/6J mice.* Ann Surg, 2004. **240**(5): p. 875-84.

119. Pittenger, G.L., et al., *Intramuscular injection of islet neogenesis-associated protein peptide stimulates pancreatic islet neogenesis in healthy dogs.* Pancreas, 2007. **34**(1): p. 103-11.

120. Dungan, K.M., J.B. Buse, and R.E. Ratner, *Effects of therapy in type 1 and type 2 diabetes mellitus with a peptide derived from islet neogenesis associated protein (INGAP).* Diabetes Metab Res Rev, 2009. **25**(6): p. 558-65.

121. Tersey, S.A., et al., *Amelioration of type 1 diabetes following treatment of non-obese diabetic mice with INGAP and lisofylline.* Journal of diabetes mellitus, 2012. **2**(2): p. 251-257.

122. Petropavlovskaia, M., et al., *Mechanisms of action of islet neogenesis-associated protein: comparison of the full-length recombinant protein and a bioactive peptide.* Am J Physiol Endocrinol Metab, 2012. **303**(7): p. E917-27.

123. Assouline-Thomas, B., et al., *Islet Neogenesis Associated Protein (INGAP) induces the differentiation of an adult human pancreatic ductal cell line into insulin-expressing cells through stepwise activation of key transcription factors for embryonic beta cell development.* Differentiation, 2015. **90**(4-5): p. 77-90.

124. Madrid, V., et al., *Islet neogenesis-associated protein (INGAP)-positive cell mass, beta-cell mass, and insulin secretion: their relationship during the fetal and neonatal periods.* Pancreas, 2013. **42**(3): p. 422-8.

125. Tam, J., L. Rosenberg, and D. Maysinger, *INGAP peptide improves nerve function and enhances regeneration in streptozotocin-induced diabetic C57BL/6 mice.* Faseb j, 2004. **18**(14): p. 1767-9.

126. Tam, J., L. Rosenberg, and D. Maysinger, *Islet-neogenesis-associated protein enhances neurite outgrowth from DRG neurons.* Biochem Biophys Res Commun, 2002. **291**(3): p. 649-54.

127. McCarthy, A.N., et al., *Islet neogenesis associated protein (ingap): structural and dynamical properties of its active pentadecapeptide.* J Mol Graph Model, 2009. **27**(6): p. 701-5.

128. Terazono, K., et al., *A novel gene activated in regenerating islets.* J Biol Chem, 1988. **263**(5): p. 2111-4.

129. Parikh, A., A.F. Stephan, and E.S. Tzanakakis, *Regenerating proteins and their expression, regulation and signaling.* Biomol Concepts, 2012. **3**(1): p. 57-70.

130. Okamoto, H., *The Reg gene family and Reg proteins: with special attention to the regeneration of pancreatic beta-cells.* J Hepatobiliary Pancreat Surg, 1999. **6**(3): p. 254-62.

131. Hamblet, N.S., et al., *The Reg family member INGAP is a marker of endocrine patterning in the embryonic pancreas.* Pancreas, 2008. **36**(1): p. 1-9.

132. Abe, M., et al., *Identification of a novel Reg family gene, Reg IIIdelta, and mapping of all three types of Reg family gene in a 75 kilobase mouse genomic region.* Gene, 2000. **246**(1-2): p. 111-22.

133. Borelli, M.I., et al., *Transcription, expression and tissue binding in vivo of INGAP and INGAP-related peptide in normal hamsters.* Regul Pept, 2007. **140**(3): p. 192-7.

134. Pittenger, G.L., D. Taylor-Fishwick, and A.I. Vinik, *The role of islet neogeneis-associated protein (INGAP) in pancreatic islet neogenesis.* Curr Protein Pept Sci, 2009. **10**(1): p. 37-45.

135. Lee, S.Y., et al., *Isolation and characterization of connective tissue progenitor cells derived from human fracture-induced hemarthrosis in vitro.* J Orthop Res, 2008. **26**(2): p. 190-9.

136. Uccelli, A., L. Moretta, and V. Pistoia, *Mesenchymal stem cells in health and disease.* Nat Rev Immunol, 2008. **8**(9): p. 726-36.

137. Owen, M., *Marrow stromal stem cells.* J Cell Sci Suppl, 1988. **10**: p. 63-76.

138. Tondreau, T., et al., *Isolation of BM mesenchymal stem cells by plastic adhesion or negative selection: phenotype, proliferation kinetics and differentiation potential.* Cytotherapy, 2004. **6**(4): p. 372-9.

139. Lindner, U., et al., *Mesenchymal Stem or Stromal Cells: Toward a Better Understanding of Their Biology?* Transfusion Medicine and Hemotherapy, 2010. **37**(2): p. 75-83.

140. Martins, L., P.K. Martin, and S.W. Han, *Angiogenic properties of mesenchymal stem cells in a mouse model of limb ischemia.* Methods Mol Biol, 2014. **1213**: p. 147-69.

141. Eliopoulos, N., et al., *Neo-organoid of marrow mesenchymal stromal cells secreting interleukin-12 for breast cancer therapy.* Cancer Res, 2008. **68**(12): p. 4810-8.

142. Eliopoulos, N., et al., *Erythropoietin delivery by genetically engineered bone marrow stromal cells for correction of anemia in mice with chronic renal failure.* J Am Soc Nephrol, 2006. **17**(6): p. 1576-84.

143. Gholamrezanezhad, A., et al., *In vivo tracking of 111In-oxine labeled mesenchymal stem cells following infusion in patients with advanced cirrhosis.* Nucl Med Biol, 2011. **38**(7): p. 961-7.

144. Thankamony, S.P. and R. Sackstein, *Enforced hematopoietic cell E- and L-selectin ligand (HCELL) expression primes transendothelial migration of human mesenchymal stem cells.* Proc Natl Acad Sci U S A, 2011. **108**(6): p. 2258-63.

145. Meleshko, A., et al., *Chimerism of allogeneic mesenchymal cells in bone marrow, liver, and spleen after mesenchymal stem cells infusion.* Pediatr Transplant, 2013. **17**(8): p. E189-94.

146. Ke, C., et al., *Migration mechanism of mesenchymal stem cells studied by QD/NSOM.* Biochim Biophys Acta, 2015. **1848**(3): p. 859-68.

147. Eliopoulos, N., et al., *Erythropoietin Gene-enhanced Marrow Mesenchymal Stromal Cells Decrease Cisplatin-induced Kidney Injury and Improve Survival of Allogeneic Mice.* Mol Ther, 2011. **19**(11): p. 2072-2083.

148. Asari, S., et al., *Mesenchymal stem cells suppress B-cell terminal differentiation.* Exp Hematol, 2009. **37**(5): p. 604-15.

149. Oh, J.Y., et al., *Mesenchymal stem/stromal cells inhibit the NLRP3 inflammasome by decreasing mitochondrial reactive oxygen species.* Stem Cells, 2014. **32**(6): p. 1553-63.

150. Todeschi, M.R., et al., *Transplanted Umbilical Cord Mesenchymal Stem Cells Modify the In Vivo Microenvironment Enhancing Angiogenesis and Leading to Bone Regeneration.* Stem Cells and Development, 2015. **24**(13): p. 1570-1581.

151. Wang, D., et al., *The regulation of the Treg/Th17 balance by mesenchymal stem cells in human systemic lupus erythematosus.* Cell Mol Immunol, 2015.

152. Jun, H.-S. and E.-Y. Park, *Adult Stem Cells as a Renewable Source of Insulin-Producing Cells.* International Journal of Stem Cells, 2009. **2**(2): p. 115-121.

153. Gabr, M.M., et al., *Insulin-producing cells from adult human bone marrow mesenchymal stem cells control streptozotocin-induced diabetes in nude mice.* Cell Transplant, 2013. **22**(1): p. 133-45.

154. Li, L., et al., *Transplantation of mesenchymal stem cells improves type 1 diabetes mellitus.* Cell Tissue Res, 2016. **364**(2): p. 345-55.

155. El-Badri, N. and M.A. Ghoneim, *Mesenchymal Stem Cell Therapy in Diabetes Mellitus: Progress and Challenges.* Journal of Nucleic Acids, 2013. **2013**: p. 194858.

156. Yaochite, J.N., et al., *Therapeutic efficacy and biodistribution of allogeneic mesenchymal stem cells delivered by intrasplenic and intrapancreatic routes in streptozotocin-induced diabetic mice.* Stem Cell Res Ther, 2015. **6**: p. 31.

157. Madec, A.M., et al., *Mesenchymal stem cells protect NOD mice from diabetes by inducing regulatory T cells.* Diabetologia, 2009. **52**(7): p. 1391-9.

158. Van Belle, T.L., P. Taylor, and M.G. von Herrath, *Mouse Models for Type 1 Diabetes.* Drug discovery today. Disease models, 2009. **6**(2): p. 41-45.

159. Tao, H., et al., *Proangiogenic Features of Mesenchymal Stem Cells and Their Therapeutic Applications.* Stem Cells International, 2016. **2016**: p. 1314709.

160. Dominici, M., et al., *Minimal criteria for defining multipotent mesenchymal stromal cells. The International Society for Cellular Therapy position statement.* Cytotherapy, 2006. **8**(4): p. 315-7.

161. Horwitz, E.M., et al., *Clarification of the nomenclature for MSC: The International Society for Cellular Therapy position statement.* Cytotherapy, 2005. **7**(5): p. 393-5.

162. Niu, T., et al., *High Efficiency Transduction of Human Mesenchymal Stem Cells Using Retroviral Gene Transfer with Triple Reporter Genes.* Blood, 2015. **104**(11): p. 4258.

163. Cooray, S., S.J. Howe, and A.J. Thrasher, *Retrovirus and lentivirus vector design and methods of cell conditioning.* Methods Enzymol, 2012. **507**: p. 29-57.

164. Sheridan, P.L., et al., *Generation of retroviral packaging and producer cell lines for large-scale vector production and clinical application: improved safety and high titer.* Mol Ther, 2000. **2**(3): p. 262-75.

165. Halim, N.S.S.A., et al., *A Comparative Study of Non-Viral Gene Delivery Techniques to Human Adipose-Derived Mesenchymal Stem Cell.* International Journal of Molecular Sciences, 2014. **15**(9): p. 15044-15060.

166. Cao, F., et al., *Comparison of gene-transfer efficiency in human embryonic stem cells.* Mol Imaging Biol, 2010. **12**(1): p. 15-24.

167. Abdi, R., et al., *Immunomodulation by mesenchymal stem cells: a potential therapeutic strategy for type 1 diabetes.* Diabetes, 2008. **57**(7): p. 1759-67.

168. Wisniewski, J., R. Agrawal, and J.A. Woodfolk, *Mechanisms of tolerance induction in allergic disease: integrating current and emerging concepts.* Clin Exp Allergy, 2013. **43**(2): p. 164-76.

169. Haase, C., et al., *Antigen-dependent immunotherapy of non-obese diabetic mice with immature dendritic cells.* Clin Exp Immunol, 2010. **160**(3): p. 331-9.

170. Peakman, M. and M. von Herrath, *Antigen-Specific Immunotherapy for Type 1 Diabetes: Maximizing the Potential.* Diabetes, 2010. **59**(9): p. 2087-2093.

171. da Silva Meirelles, L., A.I. Caplan, and N.B. Nardi, *In search of the in vivo identity of mesenchymal stem cells.* Stem Cells, 2008. **26**(9): p. 2287-99.

172. King, A.J.F., *The use of animal models in diabetes research.* British Journal of Pharmacology, 2012. **166**(3): p. 877-894.

173. Graham, M.L., et al., *The Streptozotocin-Induced Diabetic Nude Mouse Model: Differences between Animals from Different Sources.* Comparative Medicine, 2011. **61**(4): p. 356-360.

174. Pearson, J.A., F.S. Wong, and L. Wen, *The importance of the Non Obese Diabetic (NOD) mouse model in autoimmune diabetes.* J Autoimmun, 2016. **66**: p. 76-88.

175. Assouline-Thomas, B., et al., *Production and characterization of the recombinant Islet Neogenesis Associated Protein (rINGAP).* Protein Expr Purif, 2010. **69**(1): p. 1-8.

176. Vugmeyster, Y., et al., *Pharmacokinetics and toxicology of therapeutic proteins: Advances and challenges.* World Journal of Biological Chemistry, 2012. **3**(4): p. 73-92.

177. Ribeiro, S., et al., *Plasmid DNA size does affect nonviral gene delivery efficiency in stem cells.* Cell Reprogram, 2012. **14**(2): p. 130-7.

178. Castellarin, M.L., et al., *The identification and sequence analysis of a new Reg3gamma and Reg2 in the Syrian golden hamster.* Biochim Biophys Acta, 2007. **1769**(9-10): p. 579-85.

179. Mohammadi, Z., et al., *Differentiation of adipocytes and osteocytes from human adipose and placental mesenchymal stem cells.* Iranian Journal of Basic Medical Sciences, 2015. **18**(3): p. 259-266.

180. Yi, Y., M. Jong Noh, and K. Hee Lee, *Current Advances in Retroviral Gene Therapy.* Current Gene Therapy, 2011. **11**(3): p. 218-228.

181. Hopp, T.P., et al., *A Short Polypeptide Marker Sequence Useful for Recombinant Protein Identification and Purification.* Nat Biotech, 1988. **6**(10): p. 1204-1210.

182. Schmidt, P.M., et al., *Taking down the FLAG! How Insect Cell Expression Challenges an Established Tag-System.* PLoS ONE, 2012. **7**(6): p. e37779.

183. Trevino, S.R., J.M. Scholtz, and C.N. Pace, *Measuring and increasing protein solubility.* J Pharm Sci, 2008. **97**(10): p. 4155-66.

184. Eliopoulos, N., et al., *A neovascularized organoid derived from retrovirally engineered bone marrow stroma leads to prolonged in vivo systemic delivery of erythropoietin in nonmyeloablated, immunocompetent mice.* Gene Ther, 2003. **10**(6): p. 478-89.

185. Miura, M., et al., *Accumulated chromosomal instability in murine bone marrow mesenchymal stem cells leads to malignant transformation.* Stem Cells, 2006. **24**(4): p. 1095-103.

186. Muntion, S., et al., *Optimisation of mesenchymal stromal cells karyotyping analysis: implications for clinical use.* Transfus Med, 2012. **22**(2): p. 122-7.

187. Boregowda, S.V. and D.G. Phinney, *Quantifiable Metrics for Predicting MSC Therapeutic Efficacy.* Journal of stem cell research & therapy, 2016. **6**(11): p. 365.

188. Salsali, A. and M. Nathan, *A review of types 1 and 2 diabetes mellitus and their treatment with insulin.* Am J Ther, 2006. **13**(4): p. 349-61.

189. Nordquist, L., F. Palm, and B.T. Andresen, *Renal and vascular benefits of C-peptide: Molecular mechanisms of C-peptide action.* Biologics : Targets & Therapy, 2008. **2**(3): p. 441-452.